MM/mp

PS/AA/ACOL/Note 84-7
17 July 1984

ACOL BEAM APERTURES

M. Martini

1. Introduction

ACOL beam envelope diagrams have been drawn to facilitate the design of machine elements such as magnet apertures, cooling tanks and vacuum chambers. They have been plotted with the VERSATEC equipment using a graphic software especially written for that purpose, running on CYBER computer 875 [1,2]).

The program input data is:

i - beam emittance,
ii - particle momentum
iii - characteristic functions given by optics program ORBIT [3]).

2. Description of the plots: case 1

Let us proceed to a detailed explanation of Figs. 1 to 18. The horizontal axes, scaled in metres, represent the distance along the central orbit, from an arbitrary origin. The vertical axes, scaled in millimetres, represent the radial beam widths (continuous curves) and the vertical beam heights (dashed curves). The scaling factors are left to the user's convenience (limited by the paper available on VERSATEC plotter).

In the following figure, illustrating these beam aperture diagrams, the radial beam widths α_x^+, α_x^- and the vertical beam heights α_y^+, α_y^- are plotted along the central orbit (longitudinal axis s).

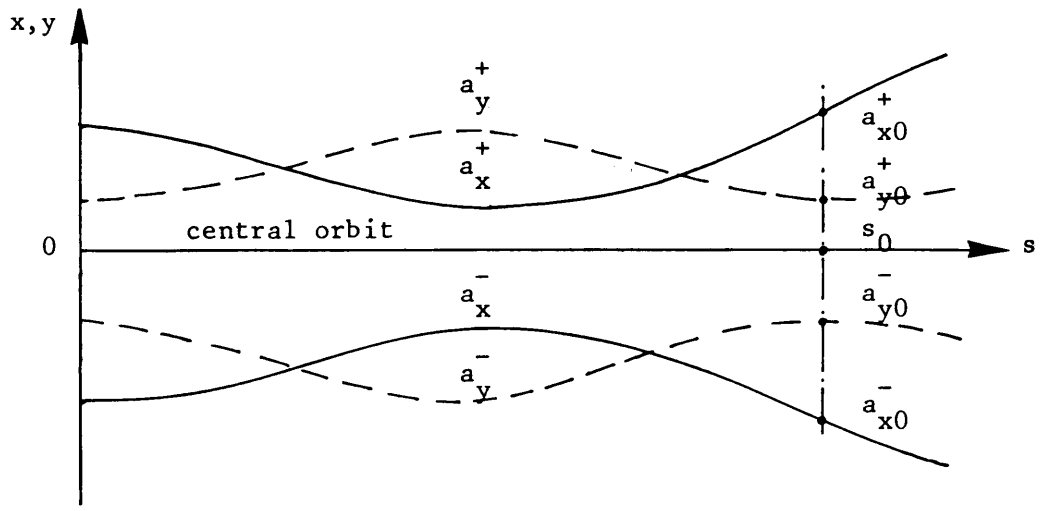

The beam sizes were calculated using the relationships:

$$a_x^+ = \sqrt{\beta_x^+ \epsilon} + x^+ \qquad a_x^- = -\sqrt{\beta_x^- \epsilon} + x^- \qquad \text{(beam widths)}$$

$$a_y^+ = \sqrt{\beta_y^+ \epsilon} \qquad a_y^- = -\sqrt{\beta_y^- \epsilon} \qquad \text{(beam heights)}$$

where

$\beta_x^+, \beta_x^-, \beta_y^+, \beta_y^-$ are the radial/vertical beta functions for $\Delta p/p$ positive and for $\Delta p/p$ negative. ($\Delta p/p = \pm 0.03$ at injection).

x^+ and x^- are the radial position of the off-momentum orbits for $\Delta p/p$ positive and negative.

ϵ is the beam emittance ($\epsilon = 240\pi$ mm.mrad at injection).

Thus, for the arcs of the machine, the beam envelope may be defined by the trapezoidal contour shown below, whose vertices are the four (x,y) coordinates: $\{(a_x^-, a_y^-)_0, (a_x^-, -a_y^-)_0, (a_x^+, -a_y^+)_0, (a_x^+, a_y^+)_0\}$. For the long straight sections, the beam cross section is a rectangle of sides $\max 2(a_x^+, -a_x^-)$, $\max 2(a_y^+, -a_y^-)$.

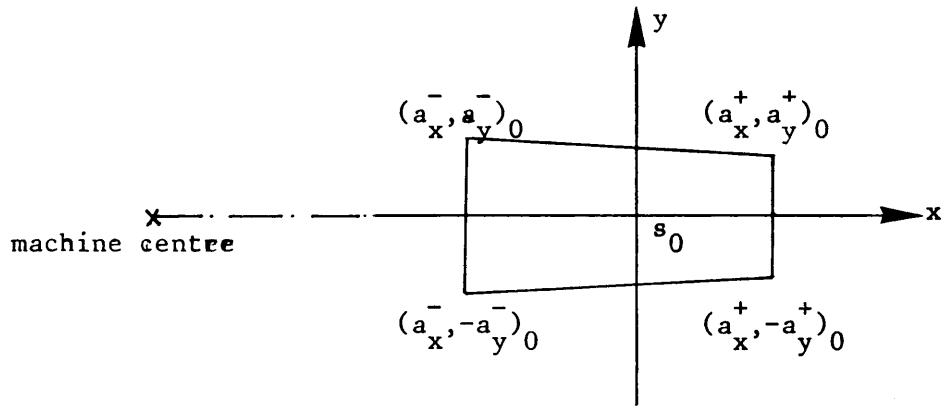

Figs 1 to 3 are plots of the first quadrant (from middle of QDN0101 to middle of QDN1501). Fig. 4 is a plot of the whole ring circumference. Figs 5 to 18 are plots of the beam apertures inside the ACOL sections 1 to 14[4]).

3. Description of the plots: case 2

This kind of plot is specific to the beam envelope inside dipoles and shifted quadrupoles. The radial beam widths (continuous curves) are defined relative to an axis (labelled z) drawn between the central orbit positions at the entrance and the exit of the dipole (or shifted quadrupole). The interpretation of vertical beam heights (dashed curves) is unchanged. The curved path of central orbit is also plotted (dashed/dotted curve). The beam size axes are scaled in millimeters, the z-axis in metres.

The main advantage of this representation over the previous one is that the beam curvature inside the magnets is visualised, allowing a proper design of vacuum chamber.

Such a beam trajectory is depicted in the figure below.

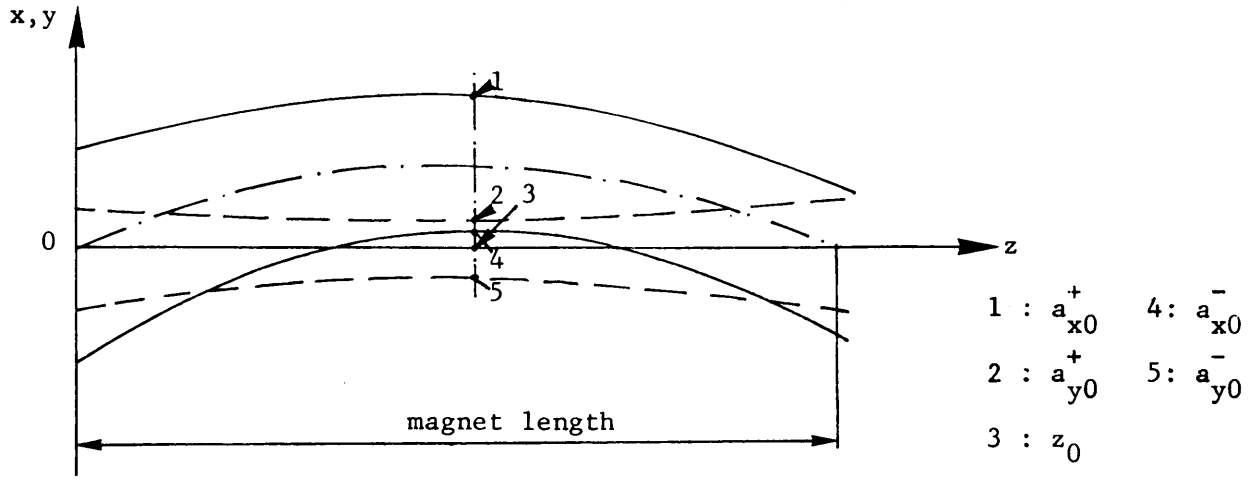

The construction of the beam envelope is similar to that described in paragraph 2.

Figs 19 to 28 are plots of the beam apertures within dipoles BHN0507 to BHN1207 and shifted quadrupoles QFH0401, QDN0501, QDN1301 and QFH1401.

In addition, Fig. 29 shows the beam dimensions and the central orbit in the first quadrant. The horizontal and vertical axes, scaled in metres, represent the coordinates of the beam envelope around the ring. The beam sizes have been expanded ten times for clarity.

Finally, Fig. 30 shows the radial and vertical beta functions (continuous and dashed curves) along with the dispersion functions (dashed/dotted curve) in the first quadrant. All the curves are given for the central orbit ($\Delta p/p=0$).

References

1. P.M. Gygi, Ancillary Programs for MAD, LEP-TH Note 25, 1983.
2. T. Risselada, Private Communication, 1984.
3. B. Autin, M. Bell, Private Communication, 1984.
4. B. Williams, ACOL Element Numbering Scheme, PS/AA/AC/84-7.

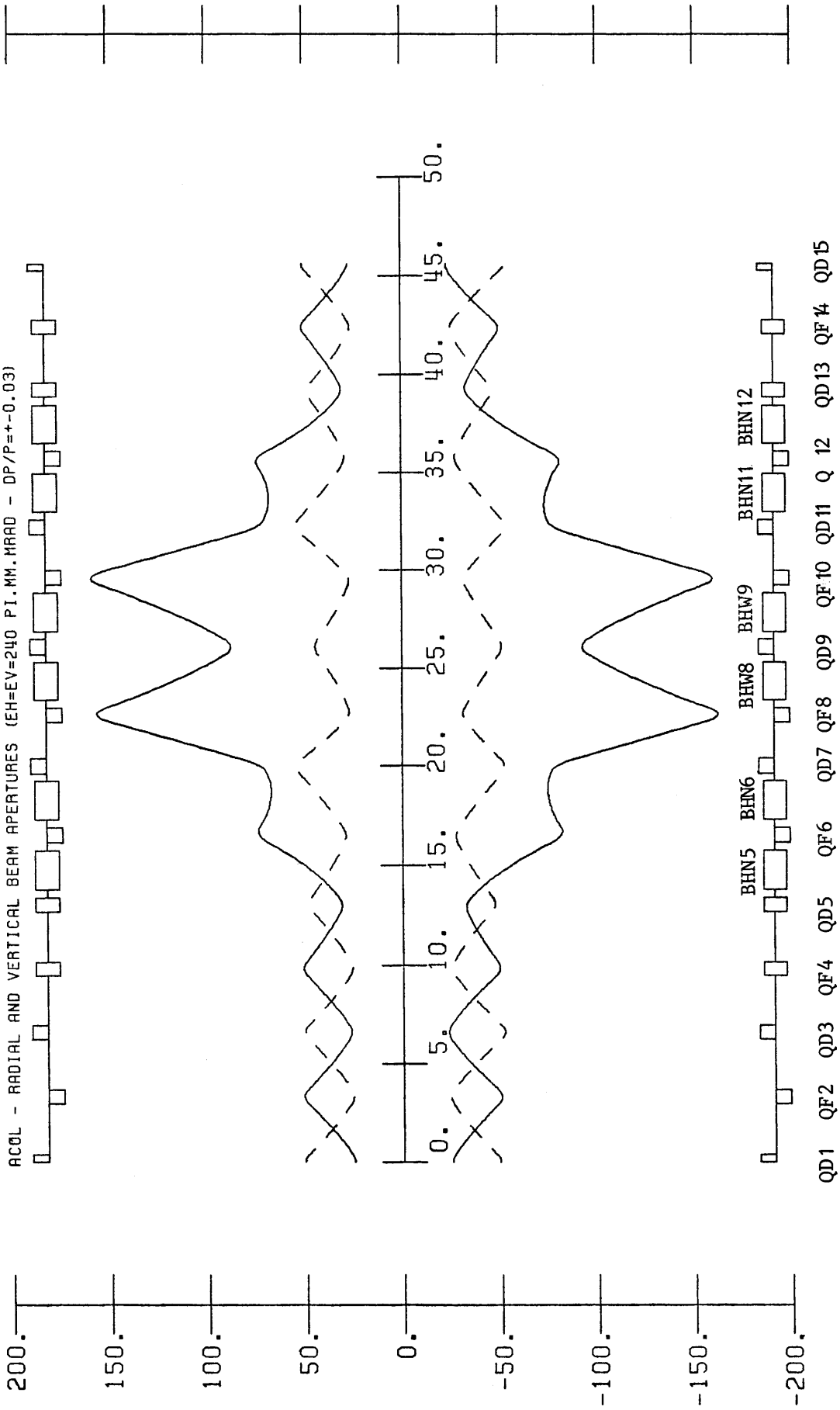

Fig. 1

Horizontal and vertical beam sizes at injection in the ACOL ring (first quadrant).

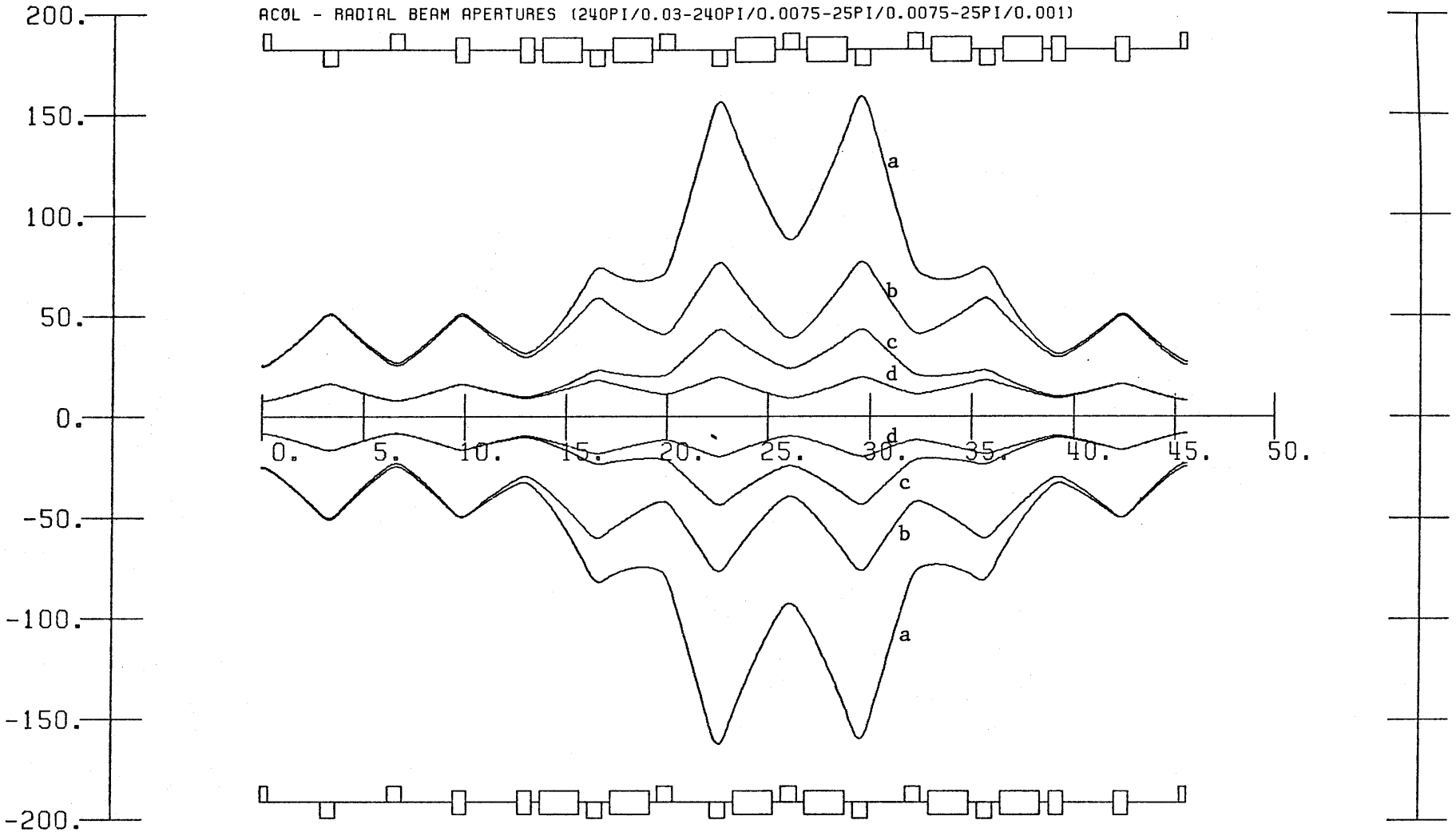

Fig. 2

Horizontal beam sizes in the ACOL ring:

a- at injection ($\epsilon = 240\pi$ - $\Delta p/p = \pm 3$ %)
b- after de-bunching ($\epsilon = 240\pi$ - $\Delta p/p = \pm 0.75$ %)
c- after betatron cooling ($\epsilon = 25\pi$ - $\Delta p/p = \pm 0.75$ %)
d- after momentum cooling ($\epsilon = 25\pi$ - $\Delta p/p = \pm 0.10$ %)

Fig. 3

Vertical beam sizes in the ACOL ring:

a- at injection ($\epsilon = 240\pi$ - $\Delta p/p = \pm 3$ %)
b- after de-bunching ($\epsilon = 240\pi$ - $\Delta p/p = \pm 0.75$ %)
c- after betatron cooling ($\epsilon = 25\pi$ - $\Delta p/p = \pm 0.75$ %)
d- after momentum cooling ($\epsilon = 25\pi$ - $\Delta p/p = \pm 0.10$ %)

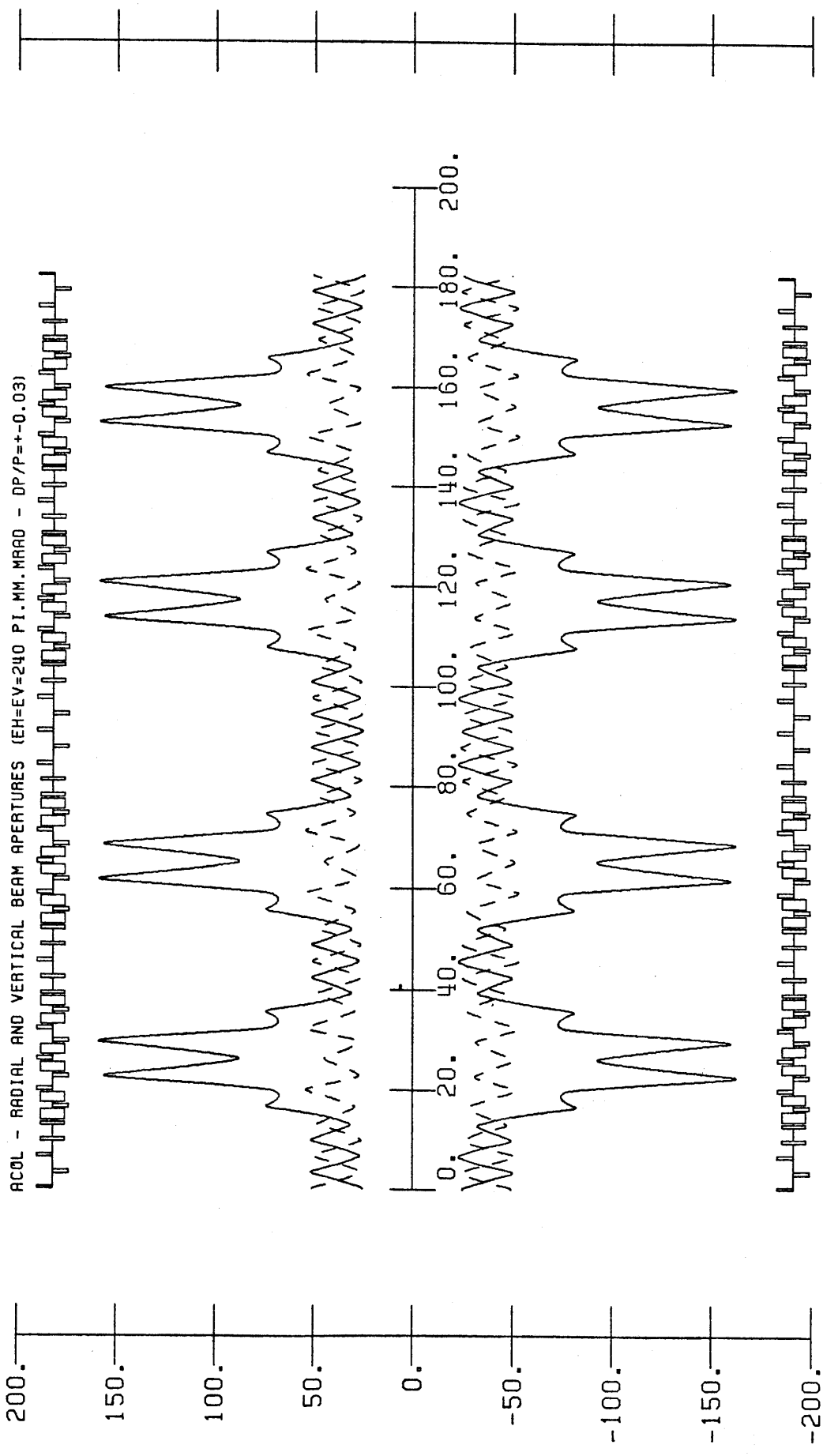

Fig. 4

Horizontal and vertical beam sizes at injection in the ACOL ring (whole circumference).

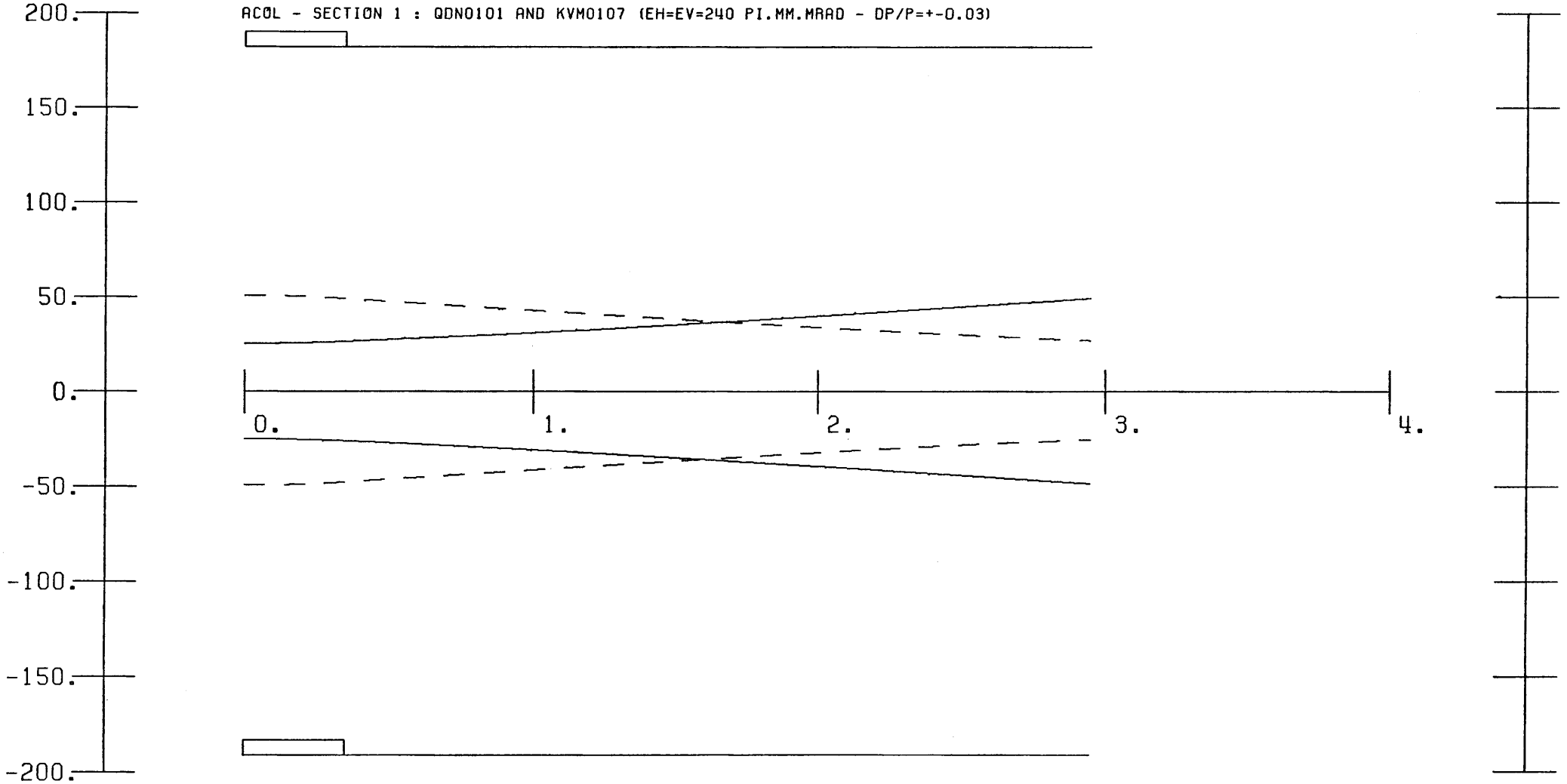
ACOL - SECTION 1 : QDN0101 AND KVM0107 (EH=EV=240 PI.MM.MRAD - DP/P=+-0.03)
200.
150.
100.
50.
0.
-50.
-100.
-150.
-200.
0.
1.
2.
3.
4.

Fig. 5

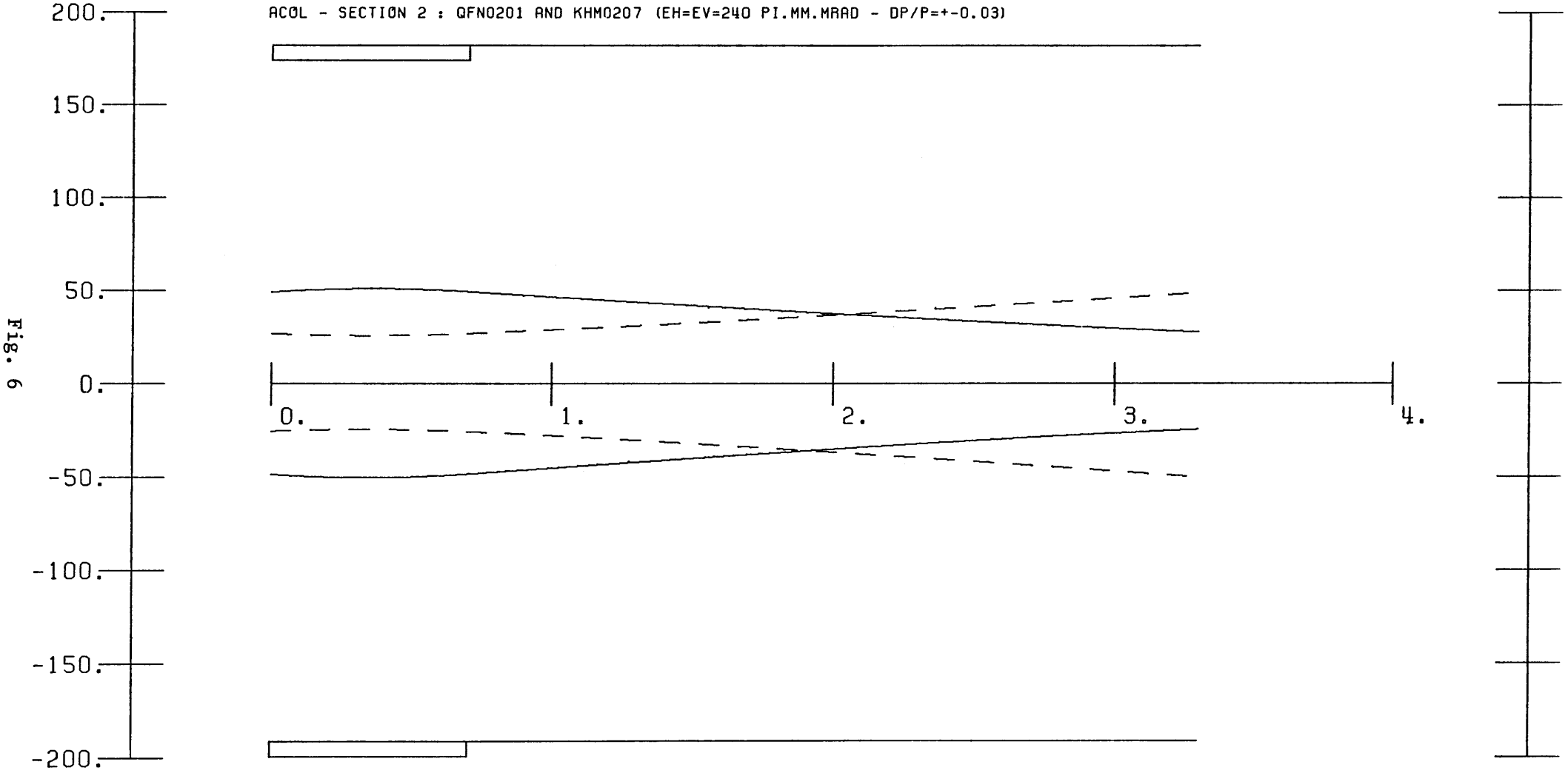
ACOL - SECTION 2 : QFN0201 AND KHM0207 (EH=EV=240 PI.MM.MRAD - DP/P=+-0.03)
200.
150.
100.
50.
0.
-50.
-100.
-150.
-200.
0.
1.
2.
3.
4.

Fig. 6

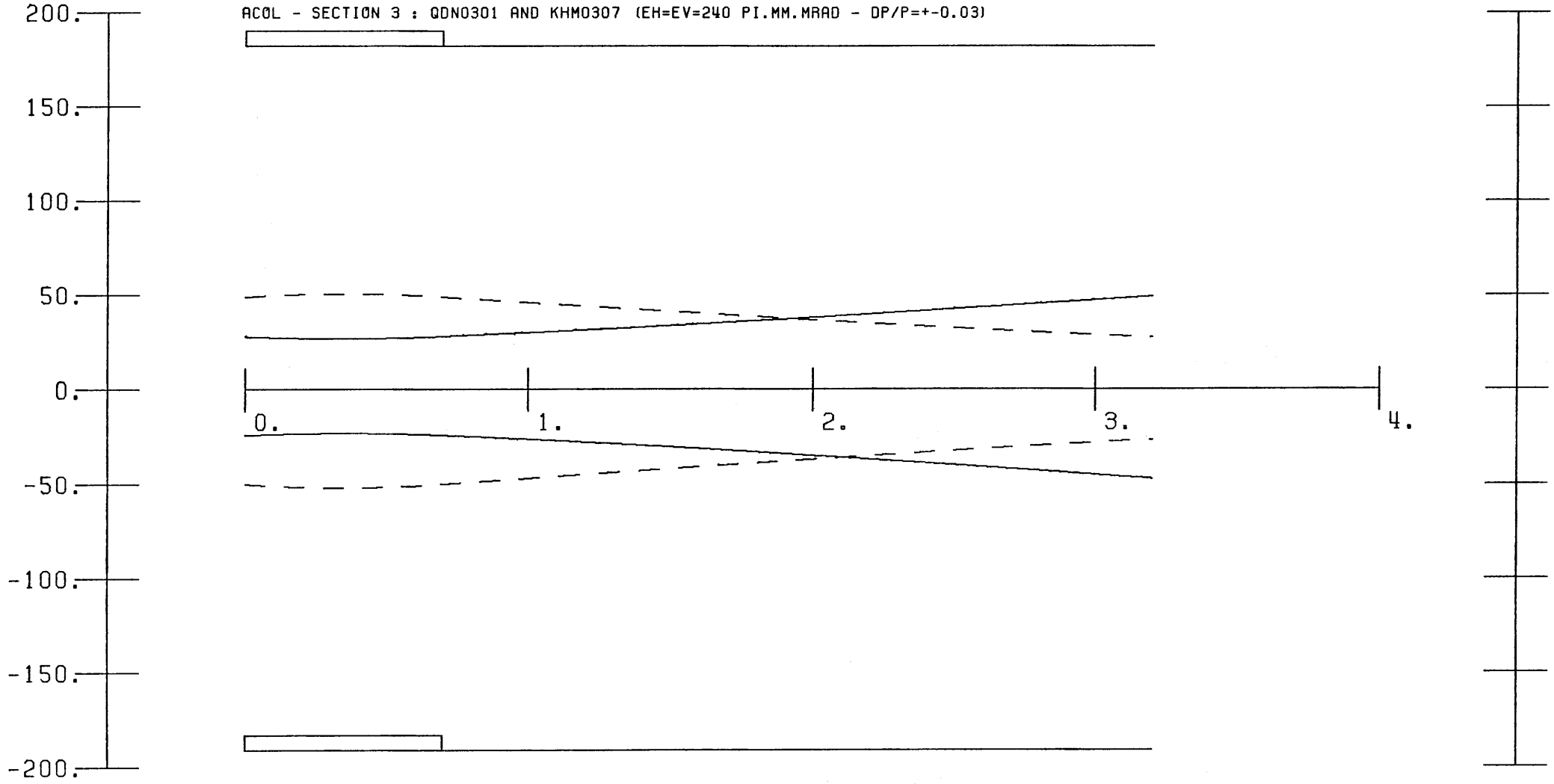
AC0L - SECTION 3 : QDN0301 AND KHM0307 (EH=EV=240 PI.MM.MRAD - DP/P=+-0.03)
200.
150.
100.
50.
0.
-50.
-100.
-150.
-200.
0.
1.
2.
3.
4.

Fig. 7

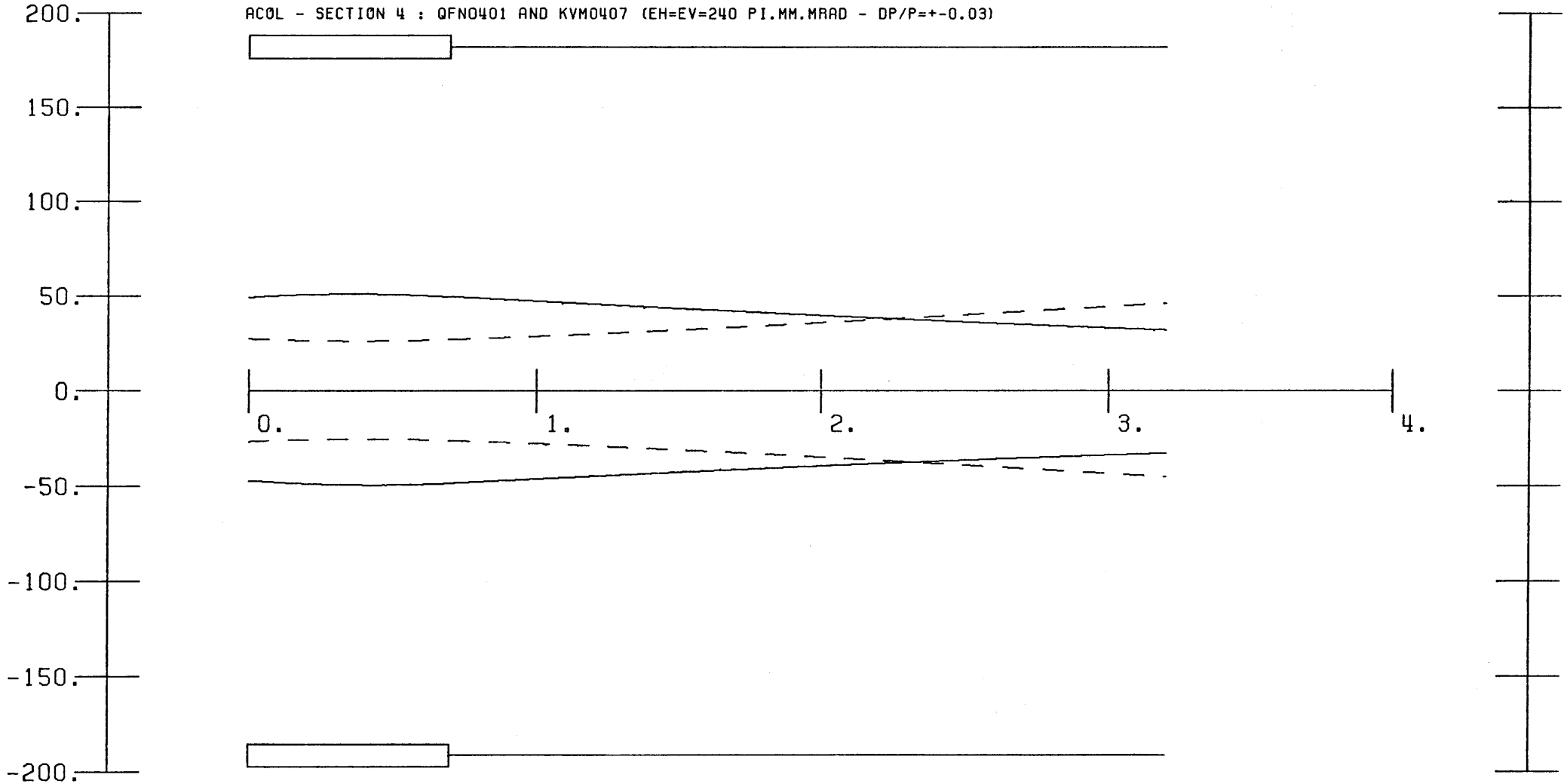
ACOL - SECTION 4 : QFNO401 AND KVMO407 (EH=EV=240 PI.MM.MRAD - DP/P=+-0.03)
200.
150.
100.
50.
0.
-50.
-100.
-150.
-200.
0.
1.
2.
3.
4.

Fig. 8

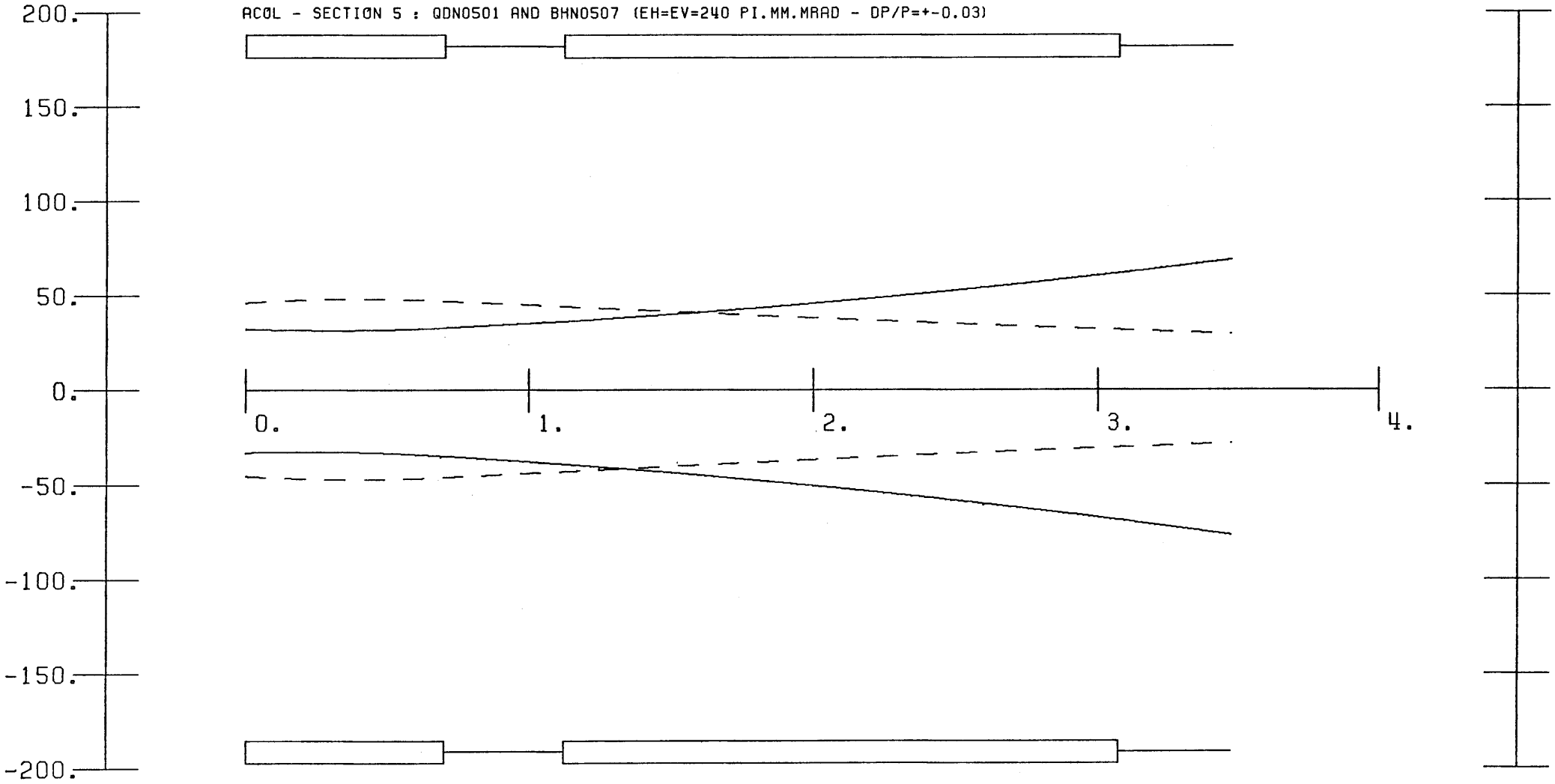
ACOL - SECTION 5 : QDN0501 AND BHN0507 (EH=EV=240 PI.MM.MRAD - DP/P=+-0.03)
200.
150.
100.
50.
0.
-50.
-100.
-150.
-200.
0.
1.
2.
3.
4.

Fig. 9

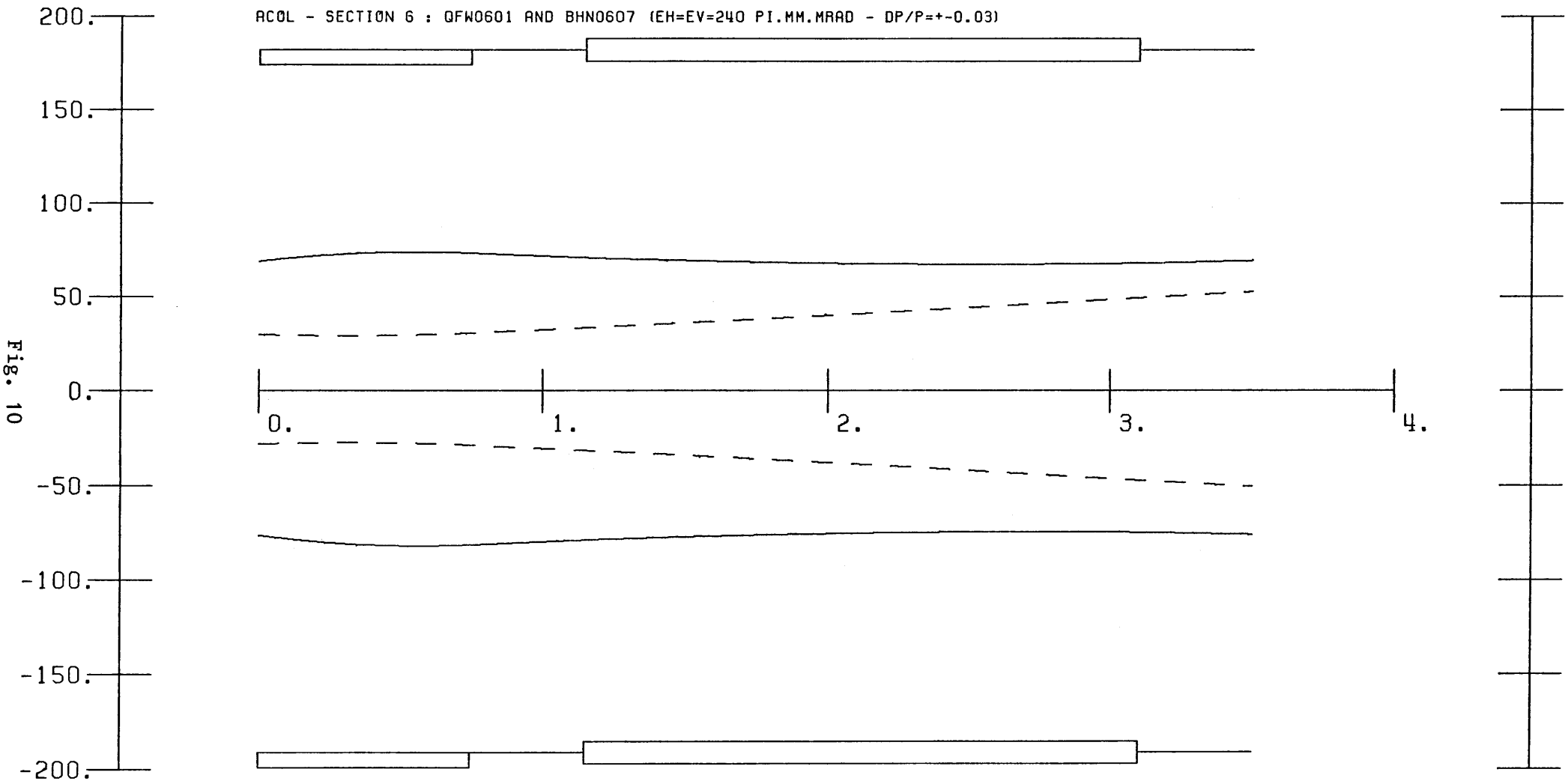
ACOL - SECTION 6 : QFW0601 AND BHN0607 (EH=EV=240 PI.MM.MRAD - DP/P=+-0.03)
200.
150.
100.
50.
0.
-50.
-100.
-150.
-200.
0.
1.
2.
3.
4.

Fig. 10

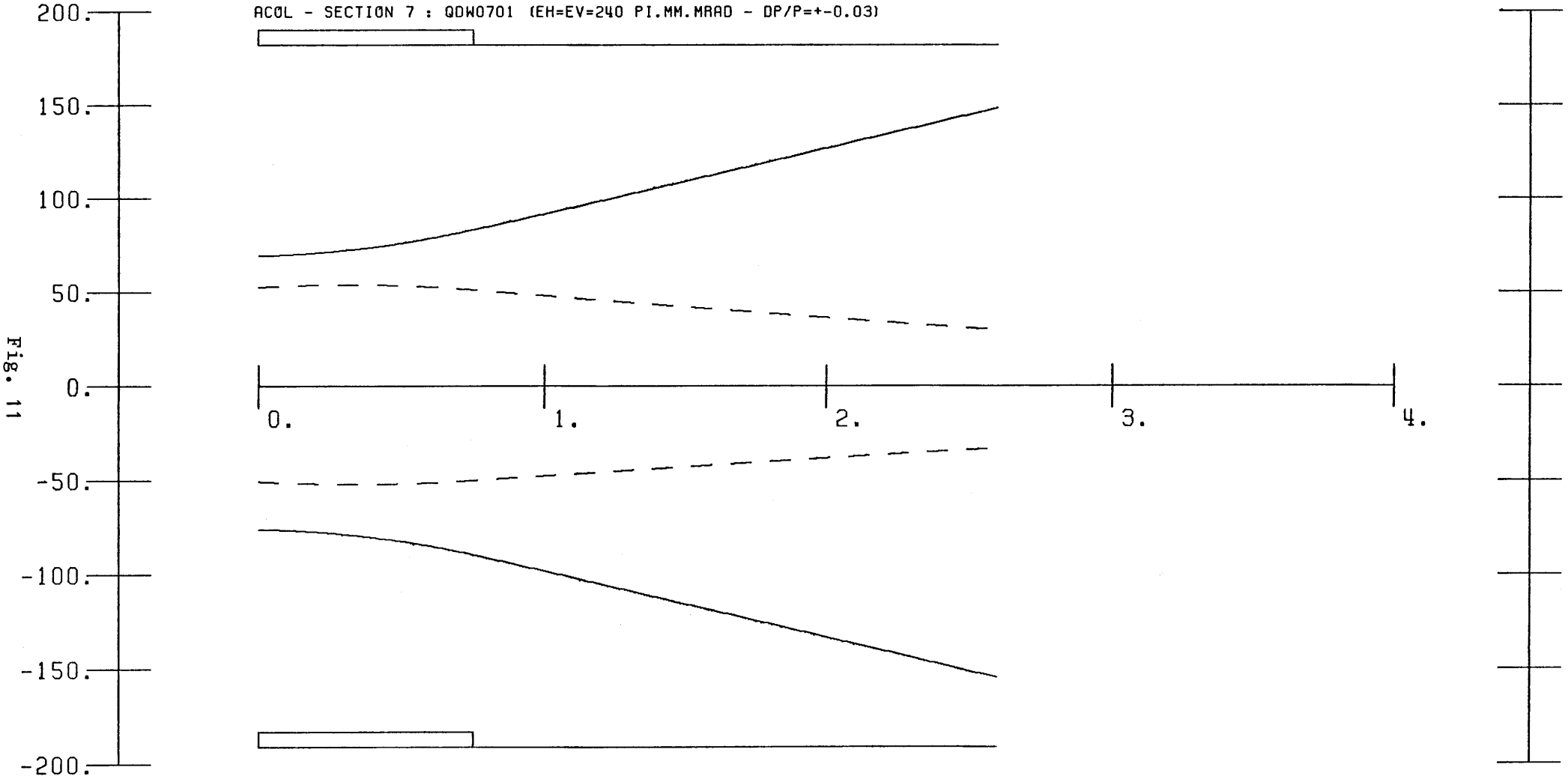
ACOL - SECTION 7 : QDW0701 (EH=EV=240 PI.MM.MRAD - DP/P=+-0.03)
200.
150.
100.
50.
0.
-50.
-100.
-150.
-200.
0.
1.
2.
3.
4.

Fig. 11

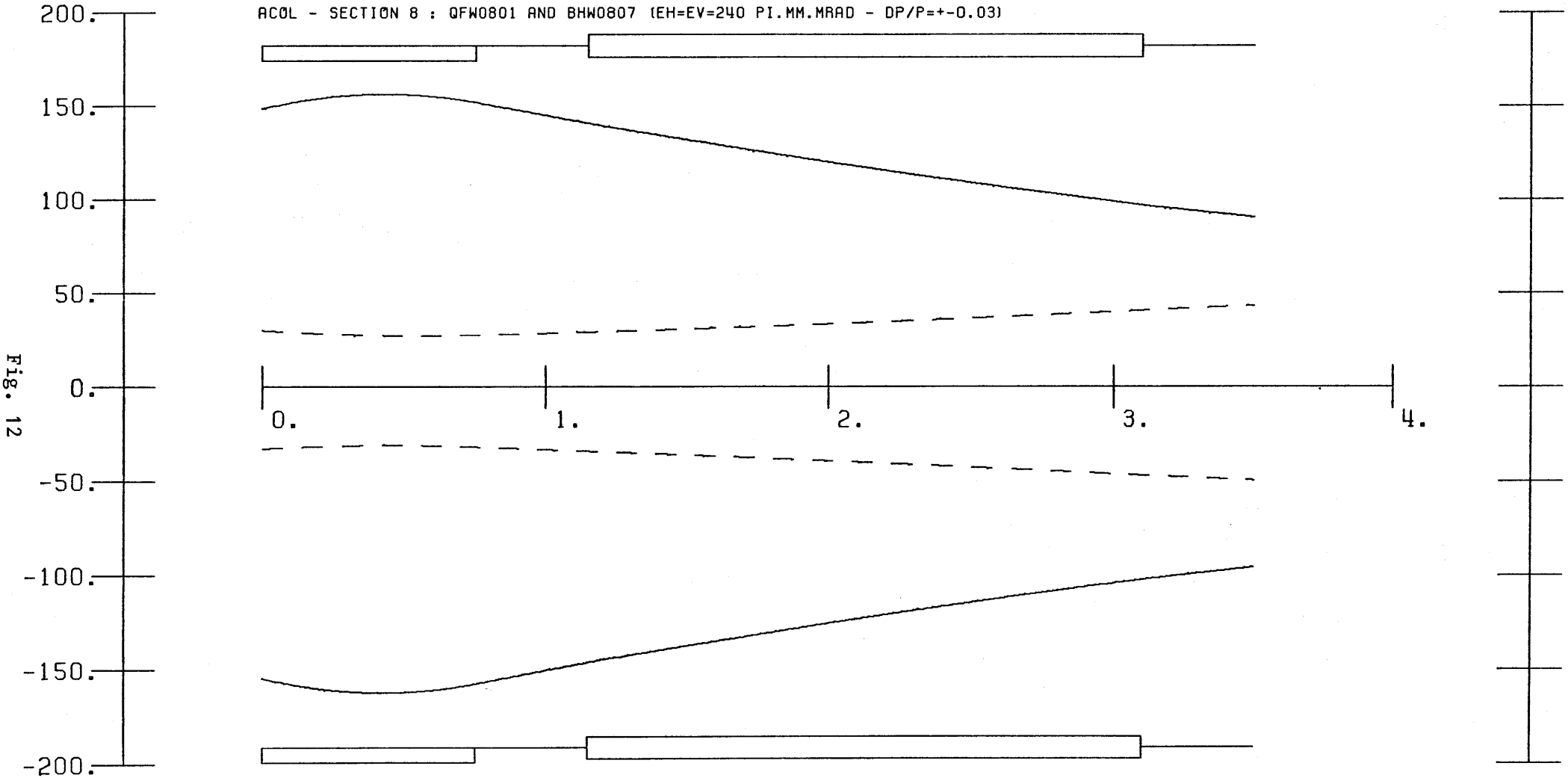
ACOL - SECTION 8 : QFW0801 AND BHW0807 (EH=EV=240 PI.MM.MRAD - DP/P=+-0.03)
200.
150.
100.
50.
0.
-50.
-100.
-150.
-200.
0.
1.
2.
3.
4.

Fig. 12

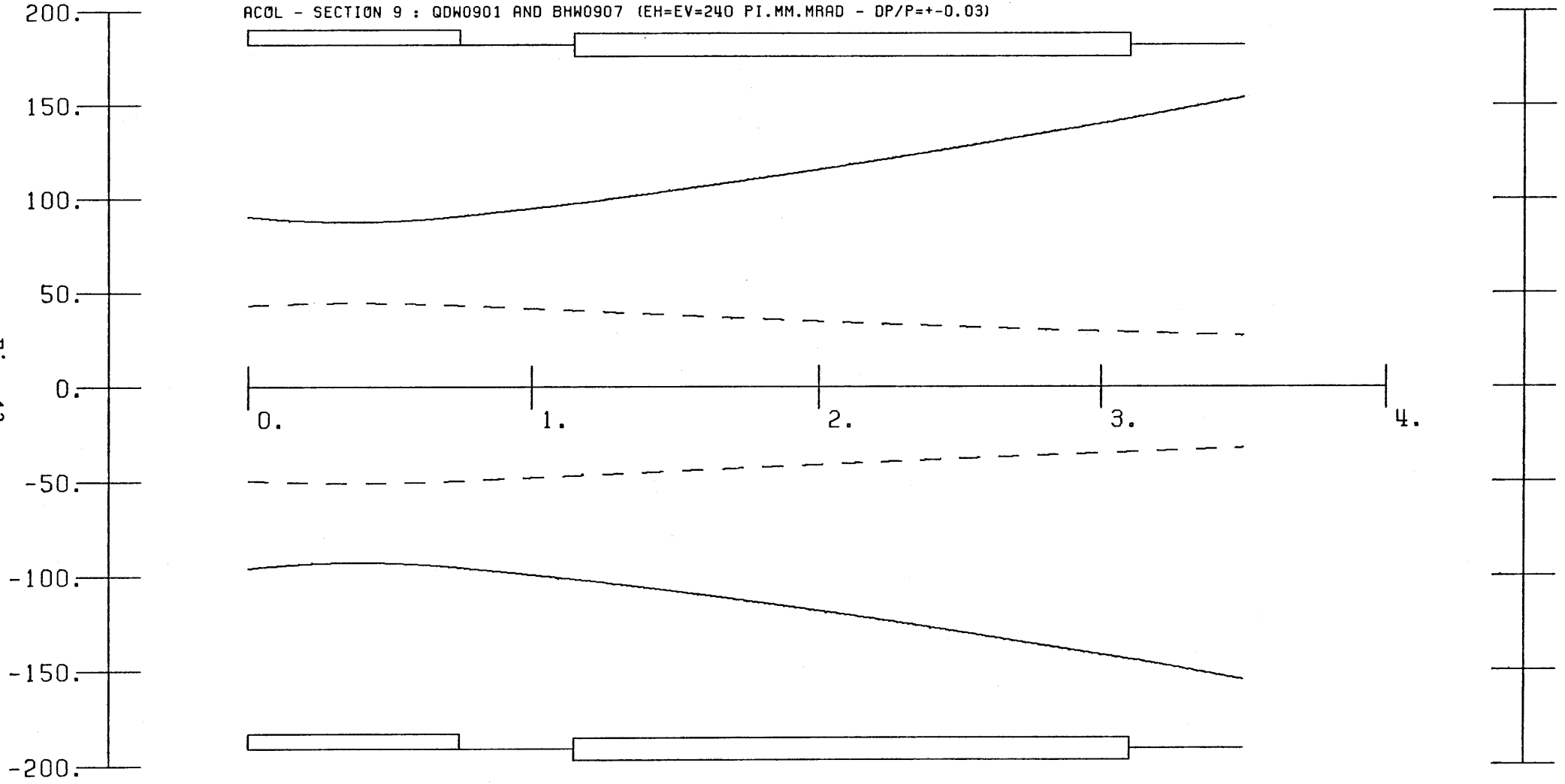
ACOL - SECTION 9 : QDW0901 AND BHW0907 (EH=EV=240 PI.MM.MRAD - DP/P=+-0.03)
200.
150.
100.
50.
0.
-50.
-100.
-150.
-200.
0.
1.
2.
3.
4.

Fig. 13

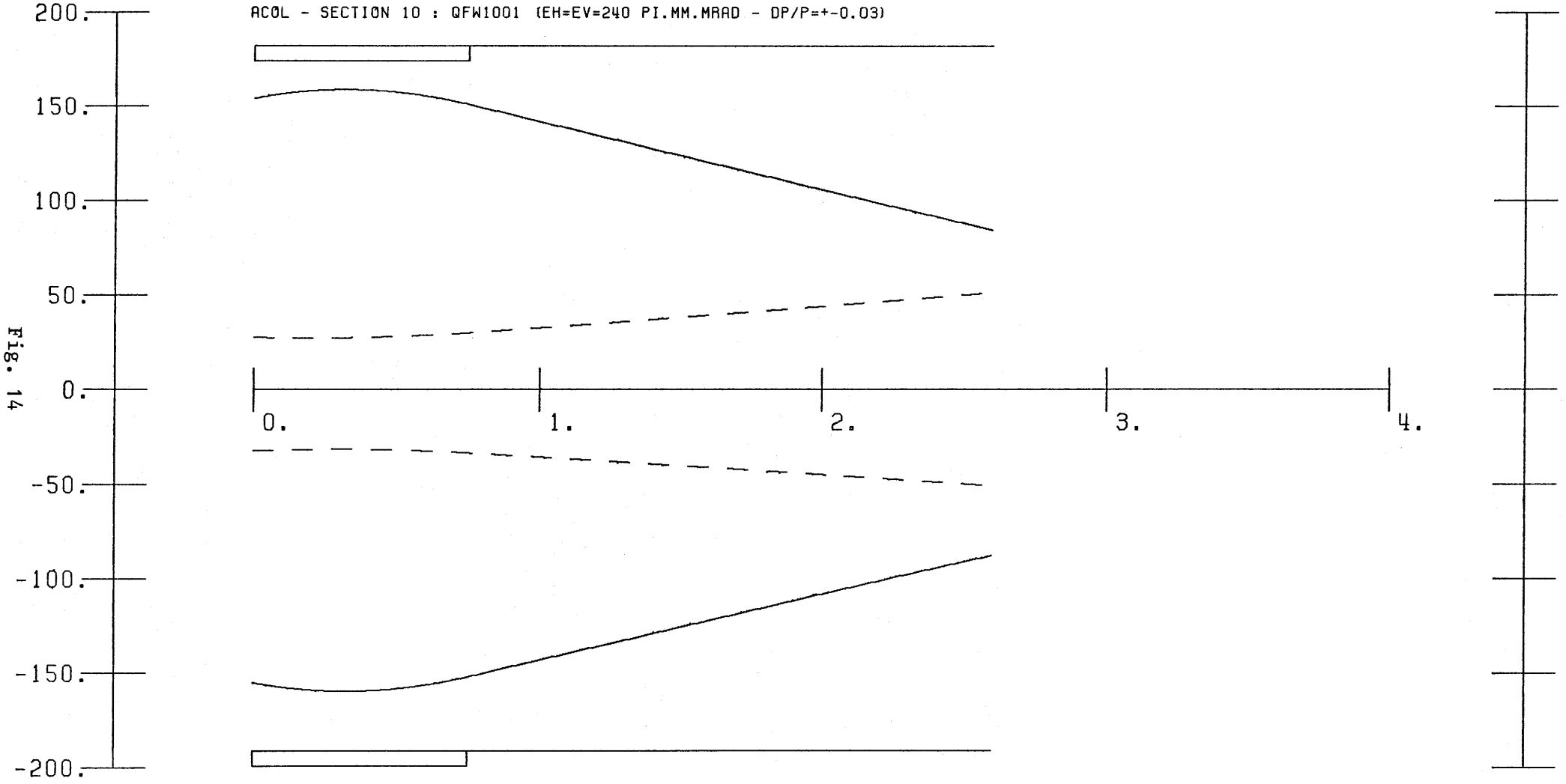
ACOL - SECTION 10 : QFW1001 (EH=EV=240 PI.MM.MRAD - DP/P=+-0.03)
200.
150.
100.
50.
0.
-50.
-100.
-150.
-200.
0.
1.
2.
3.
4.

Fig. 14

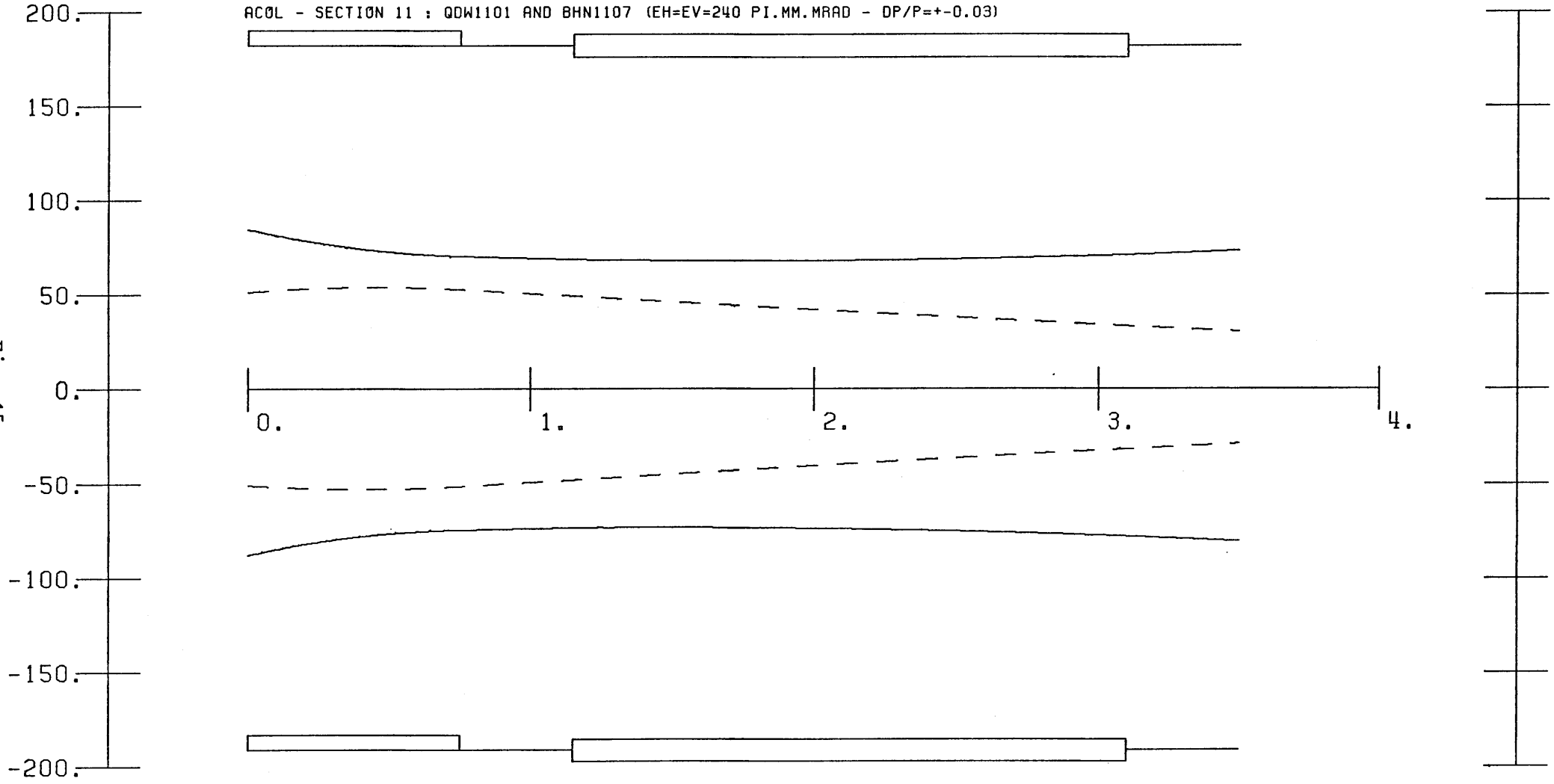
ACOL - SECTION 11 : QDW1101 AND BHN1107 (EH=EV=240 PI.MM.MRAD - DP/P=+-0.03)
200.
150.
100.
50.
0.
-50.
-100.
-150.
-200.
0.
1.
2.
3.
4.

Fig. 15

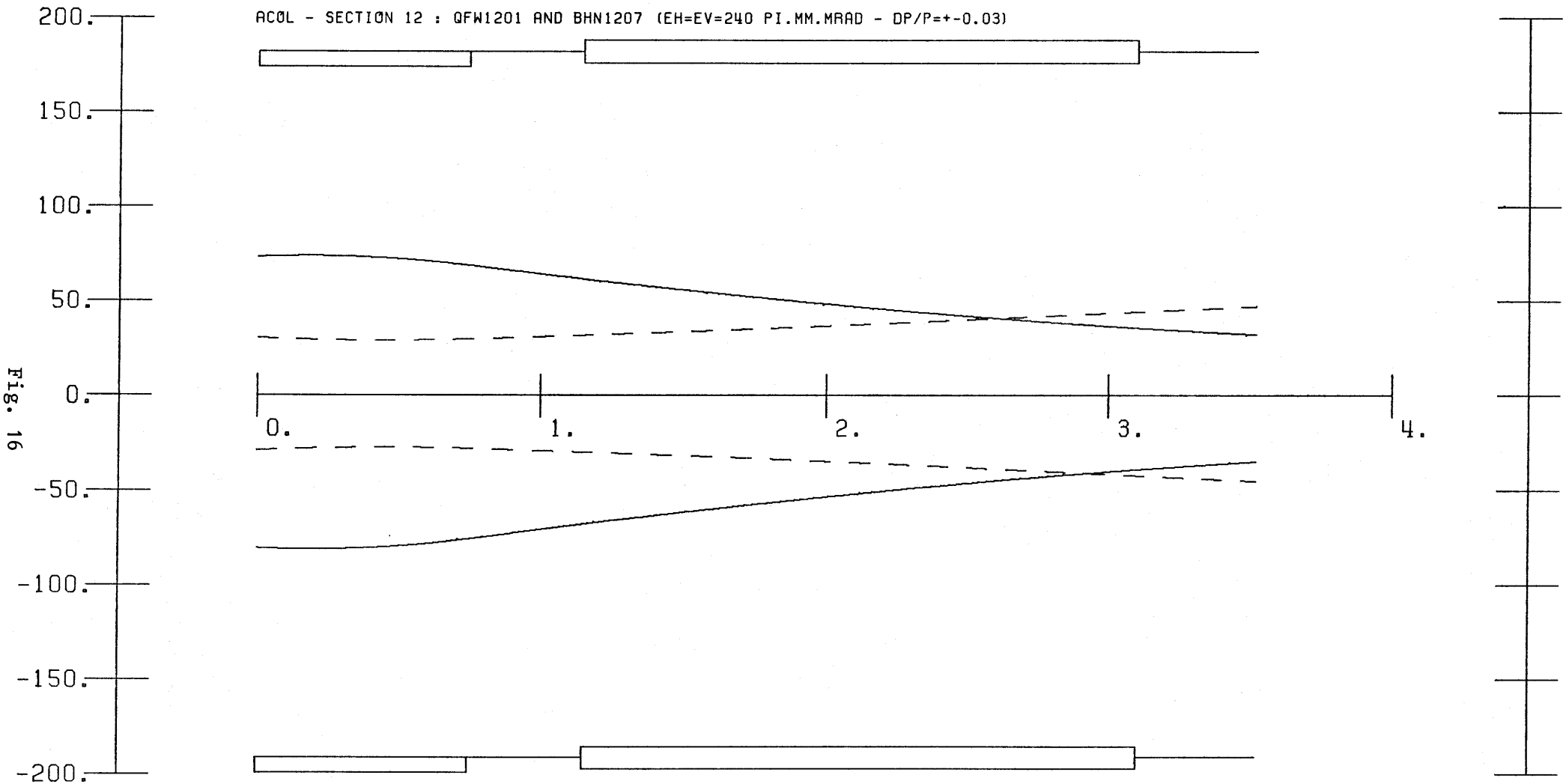
ACOL - SECTION 12 : QFW1201 AND BHN1207 (EH=EV=240 PI.MM.MRAD - DP/P=+-0.03)
200.
150.
100.
50.
0.
-50.
-100.
-150.
-200.
0.
1.
2.
3.
4.

Fig. 16

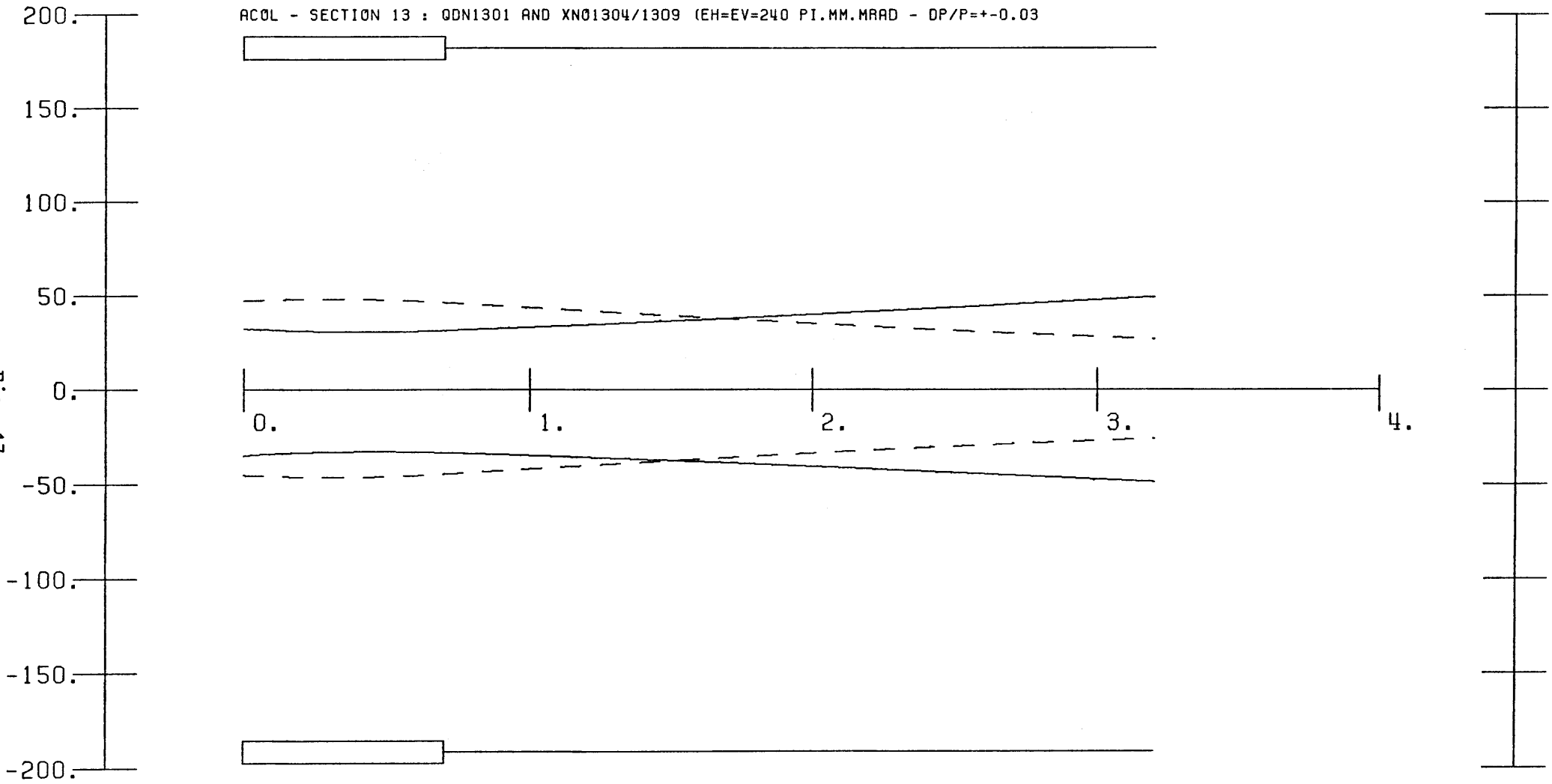
ACOL - SECTION 13 : QDN1301 AND XN01304/1309 (EH=EV=240 PI.MM.MRAD - DP/P=+-0.03
200.
150.
100.
50.
0.
-50.
-100.
-150.
-200.
0.
1.
2.
3.
4.

Fig. 17

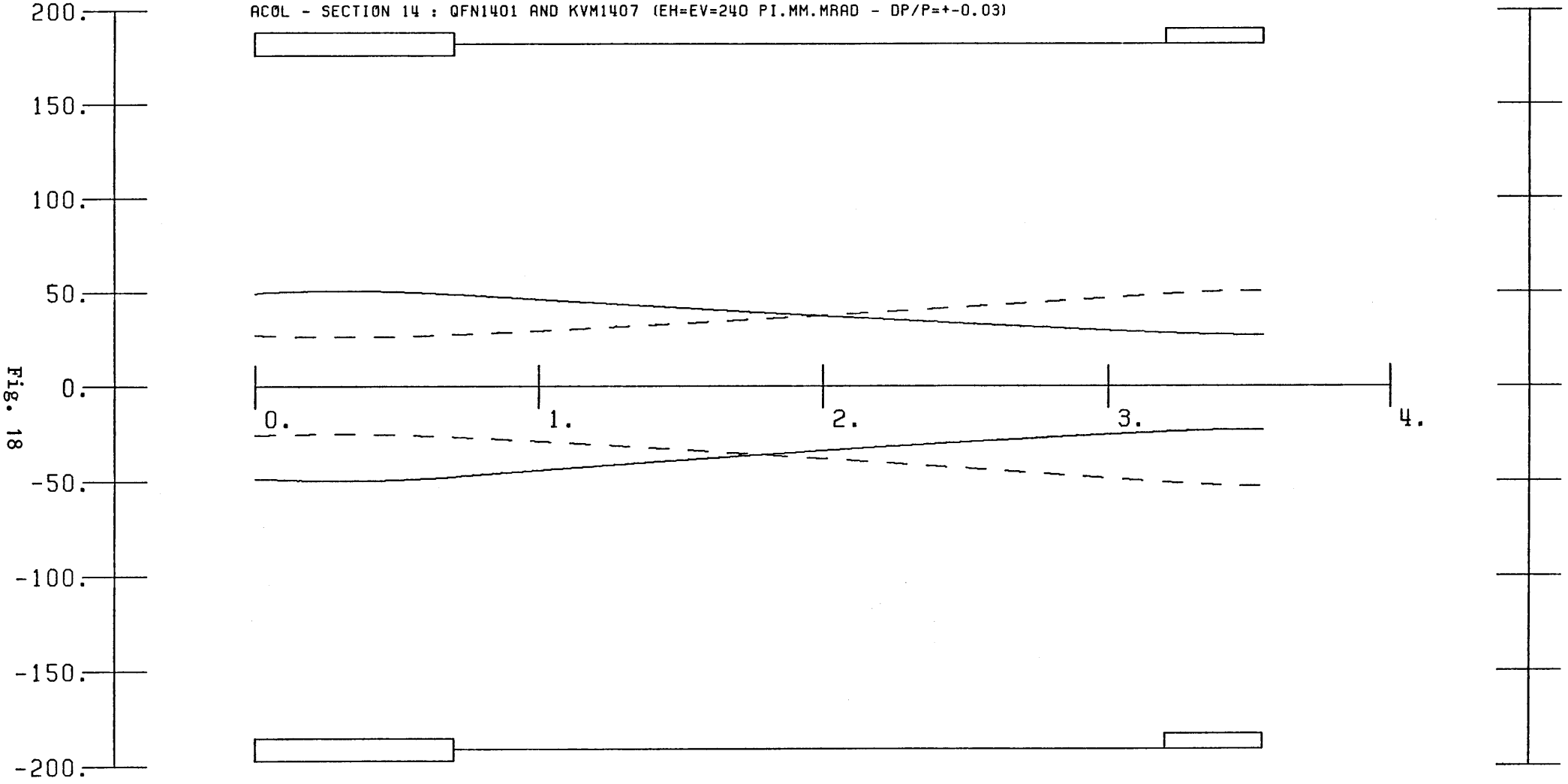
AC0L - SECTION 14 : QFN1401 AND KVM1407 (EH=EV=240 PI.MM.MRAD - DP/P=+-0.03)
200.
150.
100.
50.
0.
-50.
-100.
-150.
-200.
0.
1.
2.
3.
4.

Fig. 18

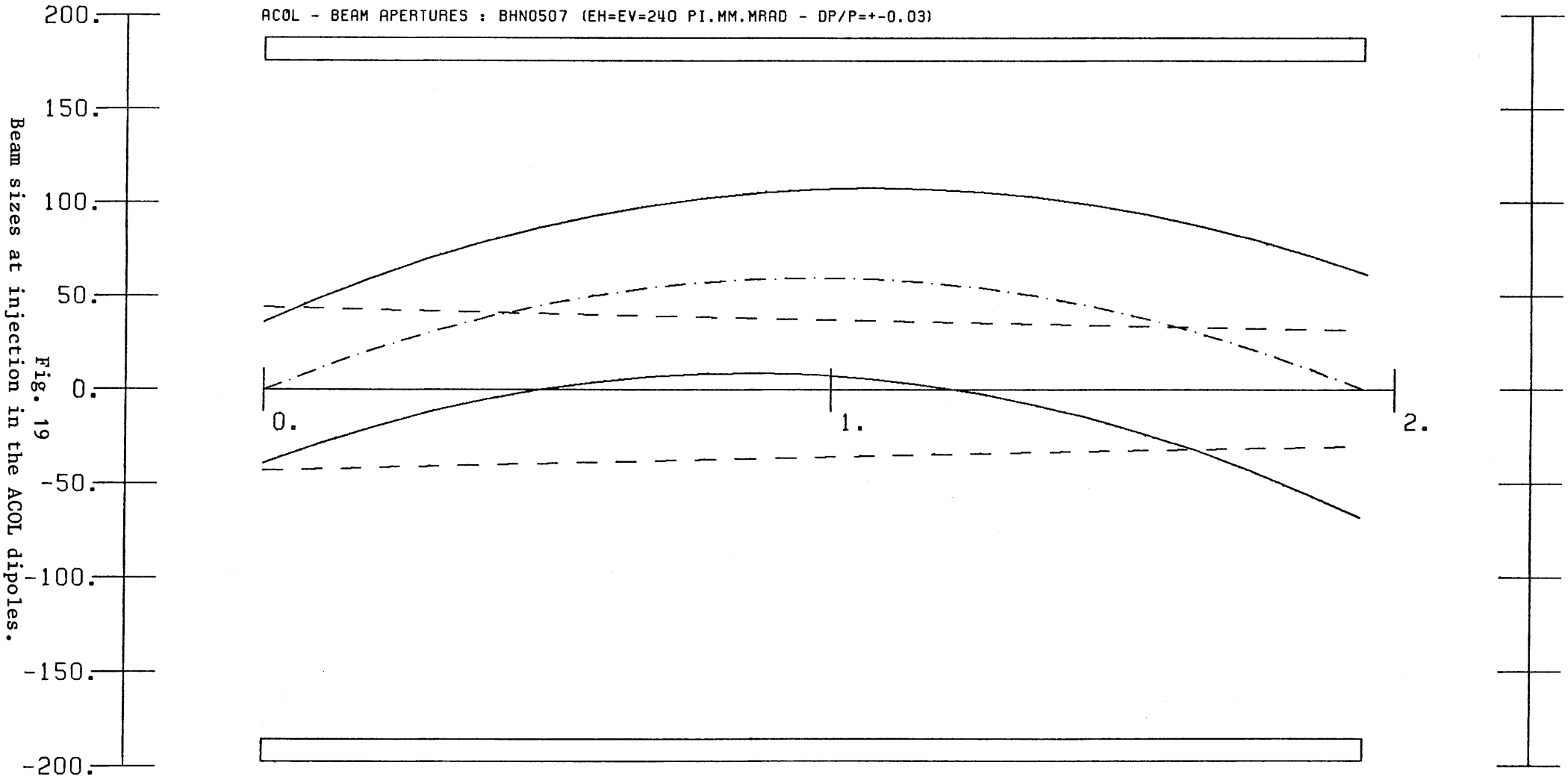

Fig. 19 Beam sizes at injection in the ACOL dipoles.

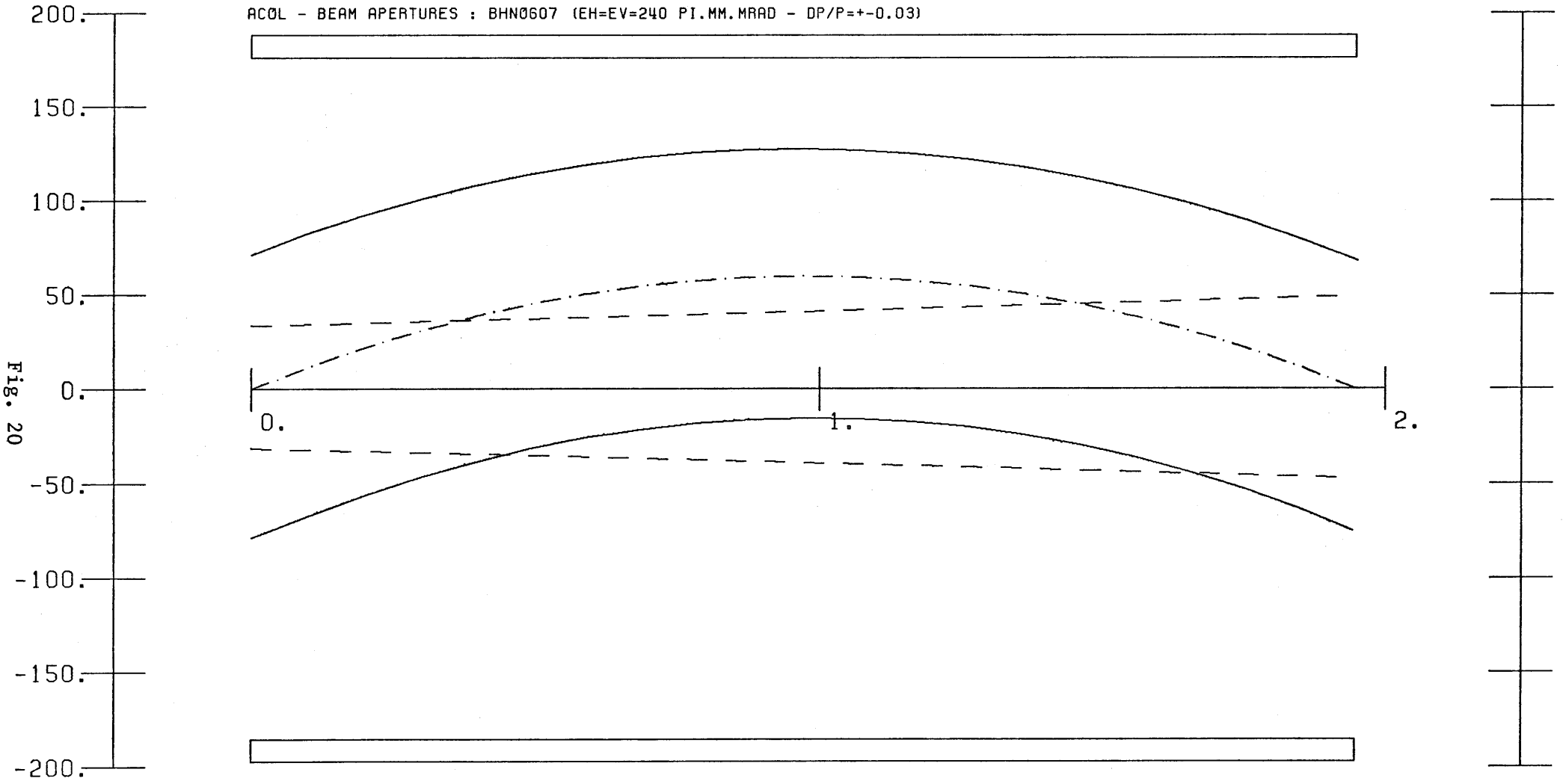
ACOL - BEAM APERTURES : BHN0607 (EH=EV=240 PI.MM.MRAD - DP/P=+-0.03)
200.
150.
100.
50.
0.
-50.
-100.
-150.
-200.
0.
1.
2.

Fig. 20

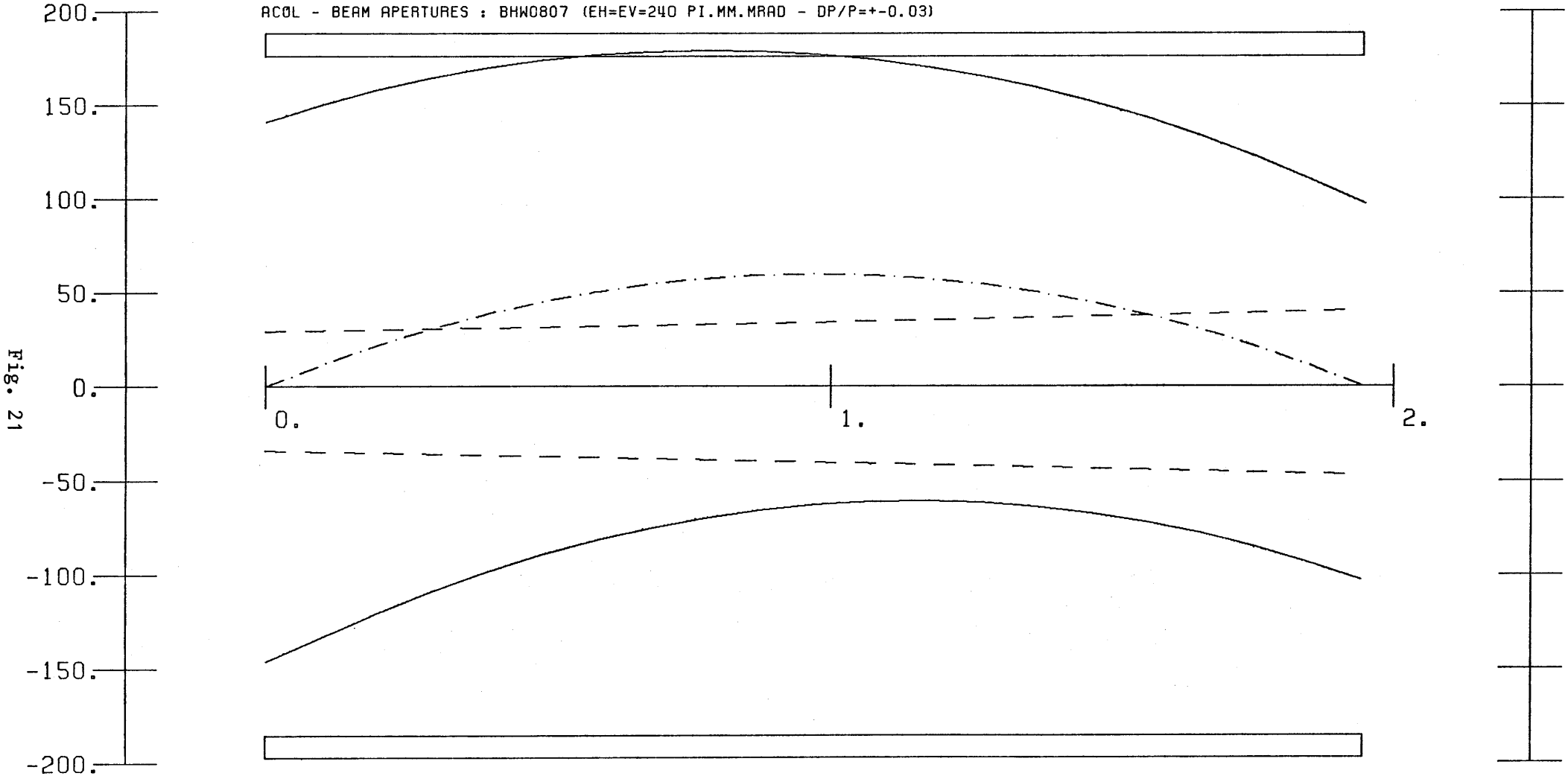
ACOL - BEAM APERTURES : BHW0807 (EH=EV=240 PI.MM.MRAD - DP/P=+-0.03)
200.
150.
100.
50.
0.
-50.
-100.
-150.
-200.
0.
1.
2.

Fig. 21

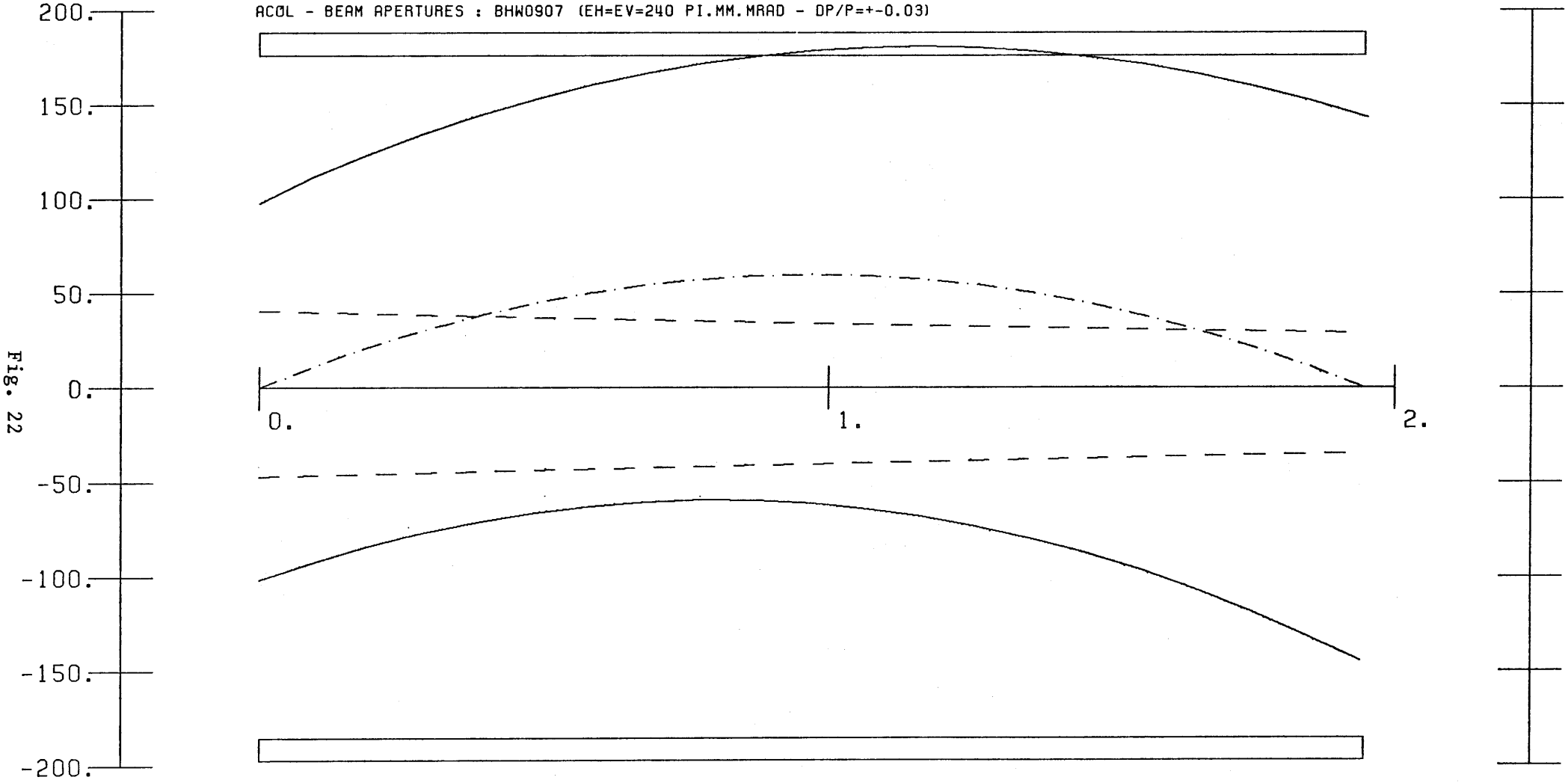
ACOL - BEAM APERTURES : BHW0907 (EH=EV=240 PI.MM.MRAD - DP/P=+-0.03)
200.
150.
100.
50.
0.
-50.
-100.
-150.
-200.
0.
1.
2.

Fig. 22

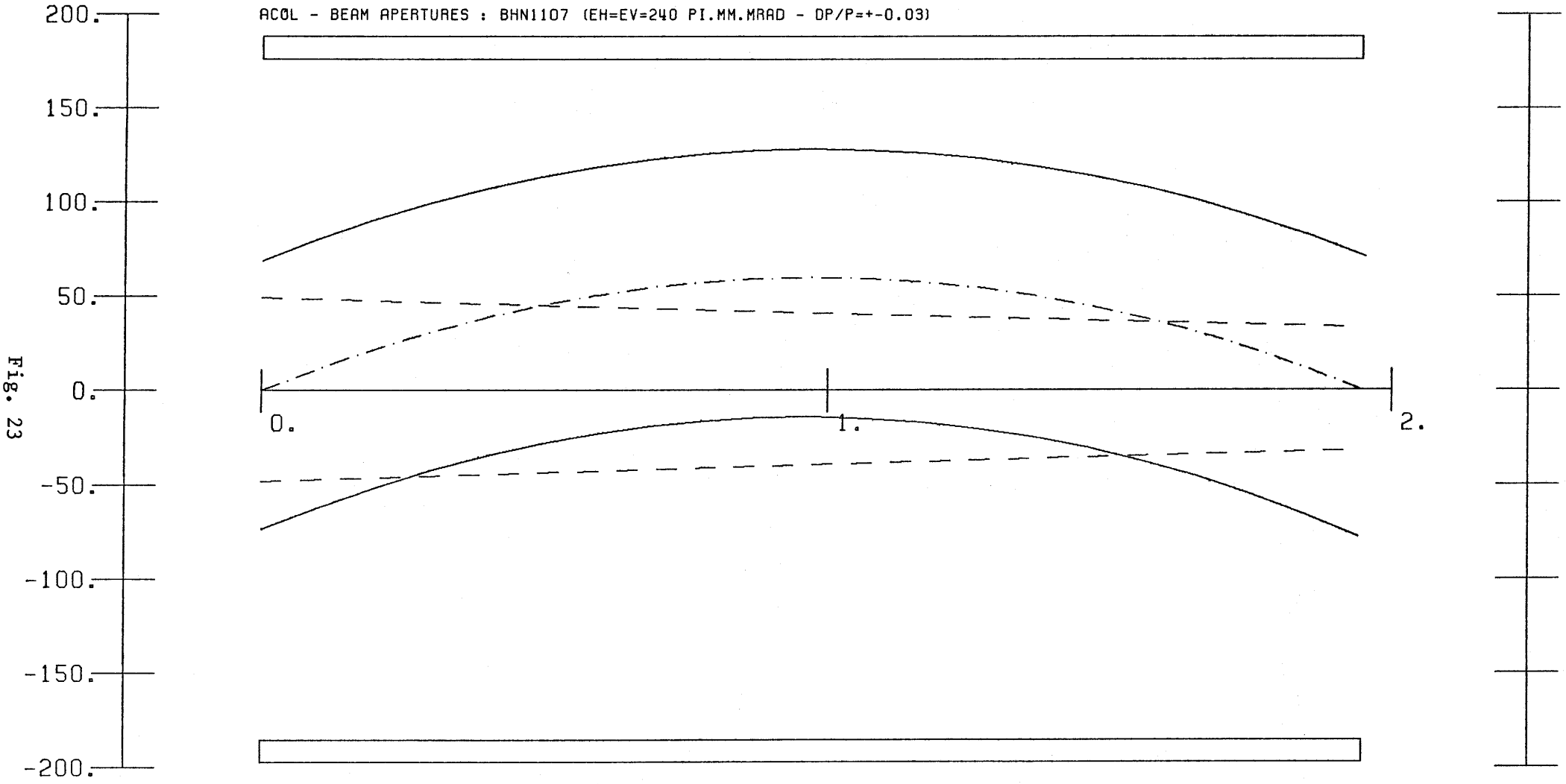
ACOL - BEAM APERTURES : BHN1107 (EH=EV=240 PI.MM.MRAD - DP/P=+-0.03)
200.
150.
100.
50.
0.
-50.
-100.
-150.
-200.
0.
1.
2.

Fig. 23

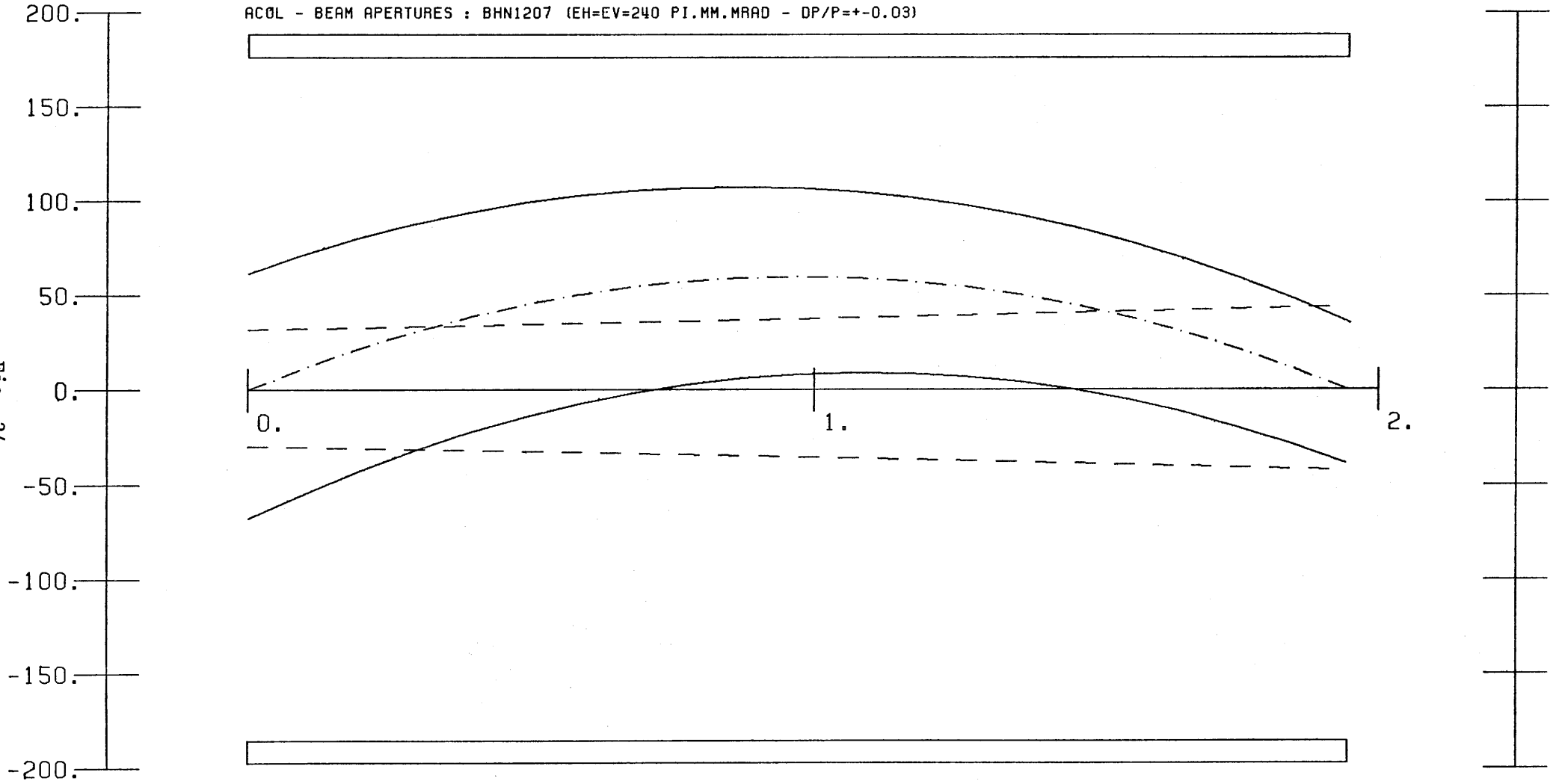
ACOL - BEAM APERTURES : BHN1207 (EH=EV=240 PI.MM.MRAD - DP/P=+-0.03)
200.
150.
100.
50.
0.
-50.
-100.
-150.
-200.
0.
1.
2.

Fig. 24

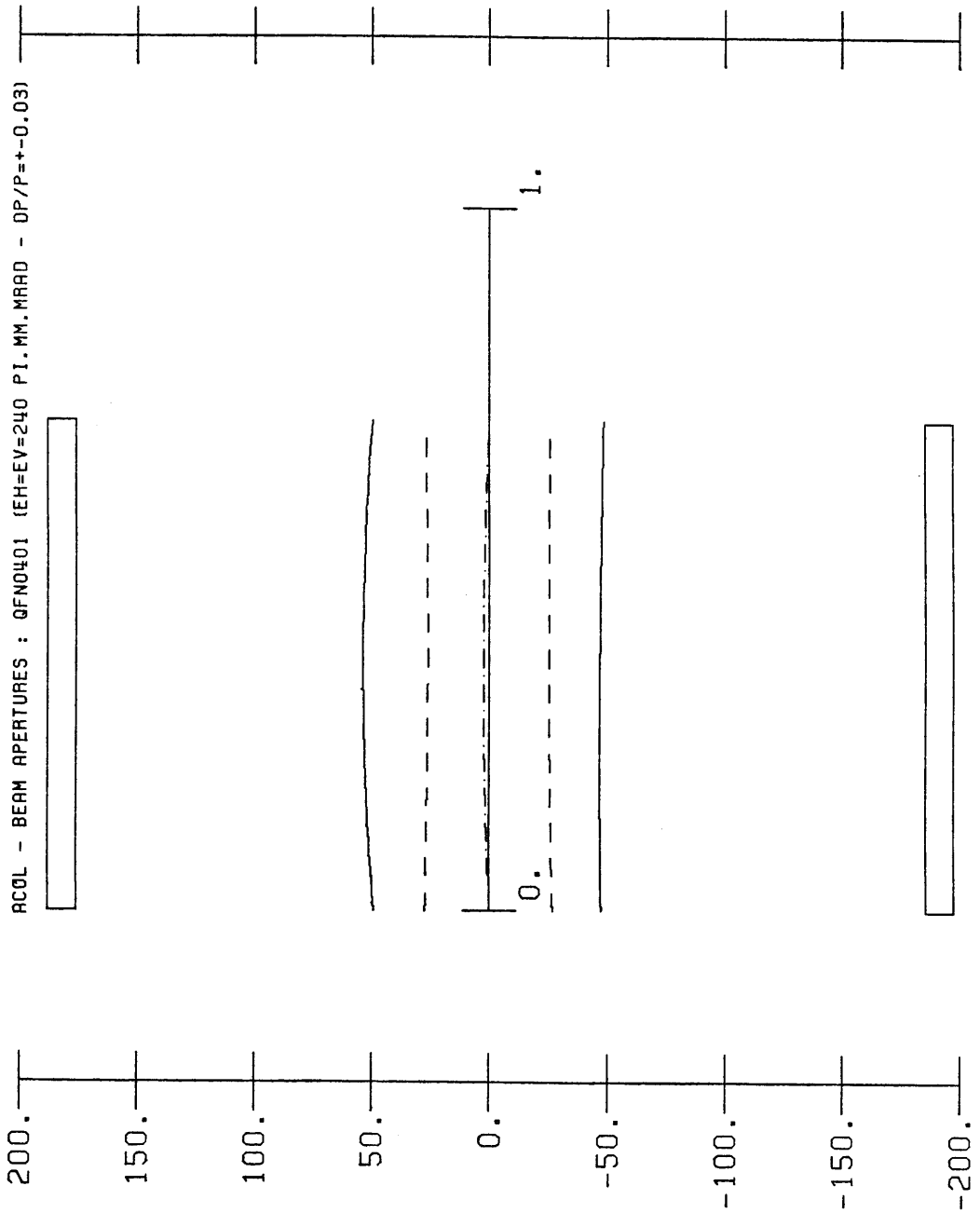

Fig. 25

Horizontal and vertical beam sizes at injection in the ACOL shifted quadrupoles.

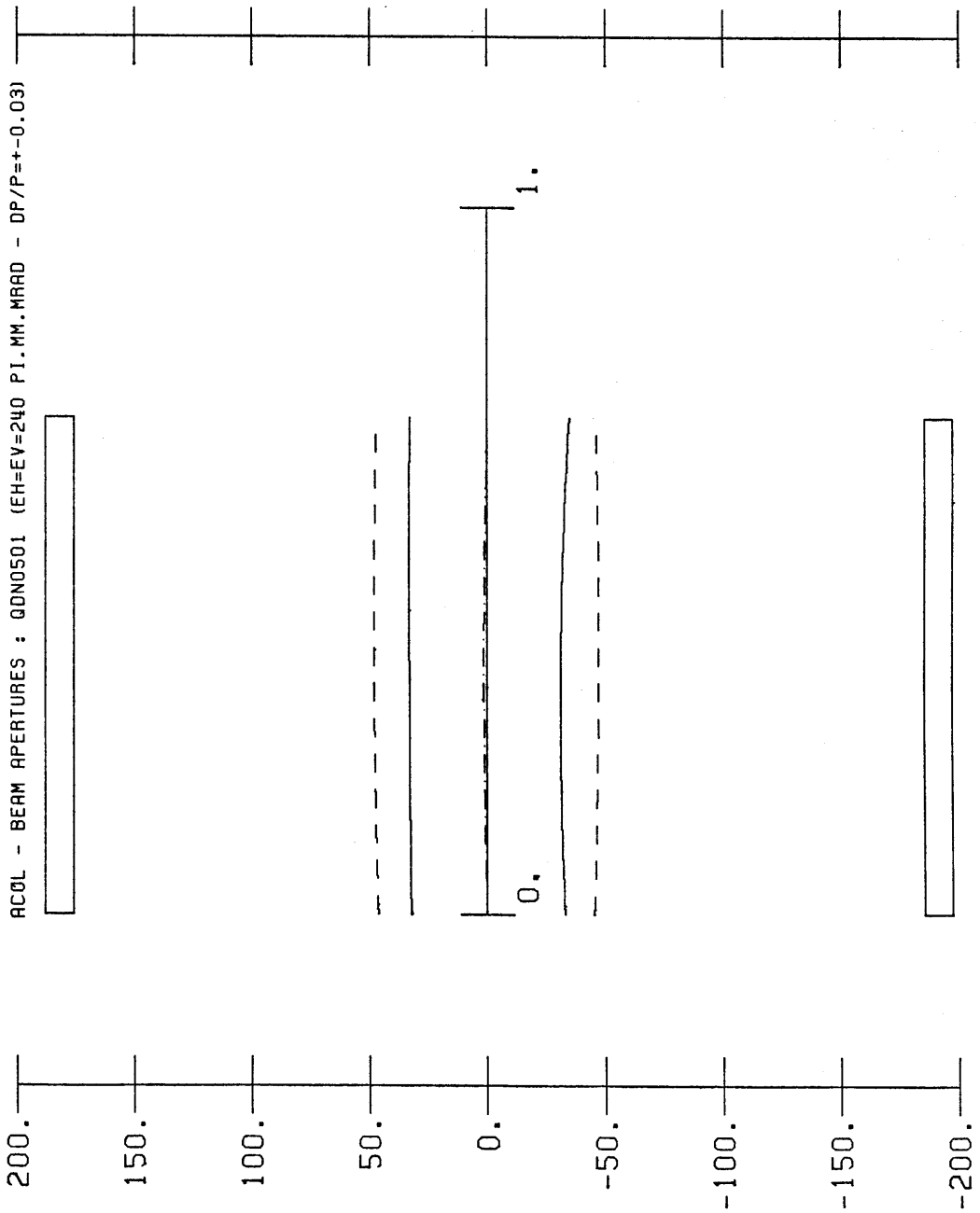
ACOL - BEAM APERTURES : QDNO501 (EH=EV=240 PI.MM.MRAD - DP/P=+-0.03)
1.
0.
200.
150.
100.
50.
0.
-50.
-100.
-150.
-200.

Fig. 26

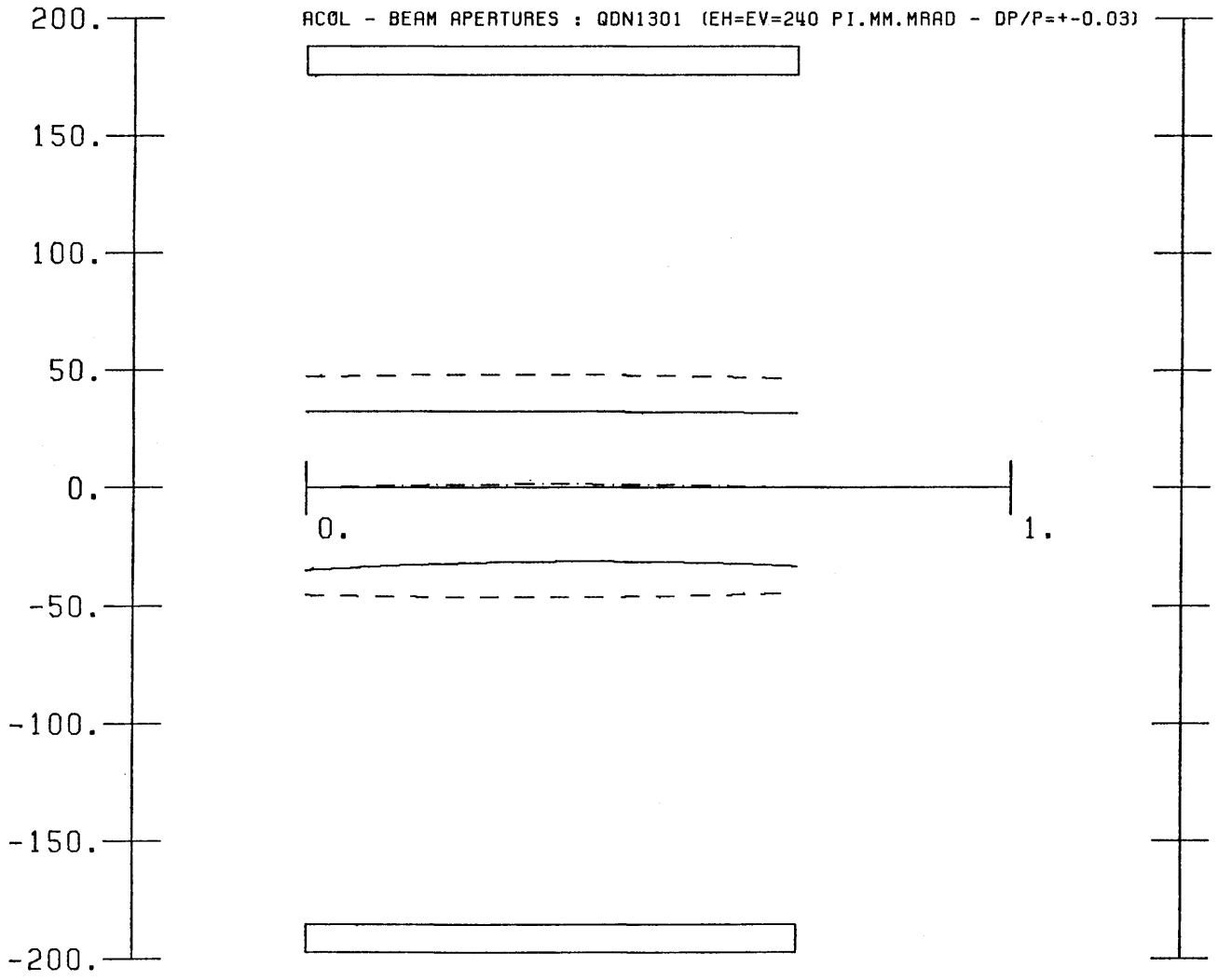
ACOL - BEAM APERTURES : QDN1301 (EH=EV=240 PI.MM.MRAD - DP/P=+-0.03)
200.
150.
100.
50.
0.
-50.
-100.
-150.
-200.
0.
1.

Fig. 27

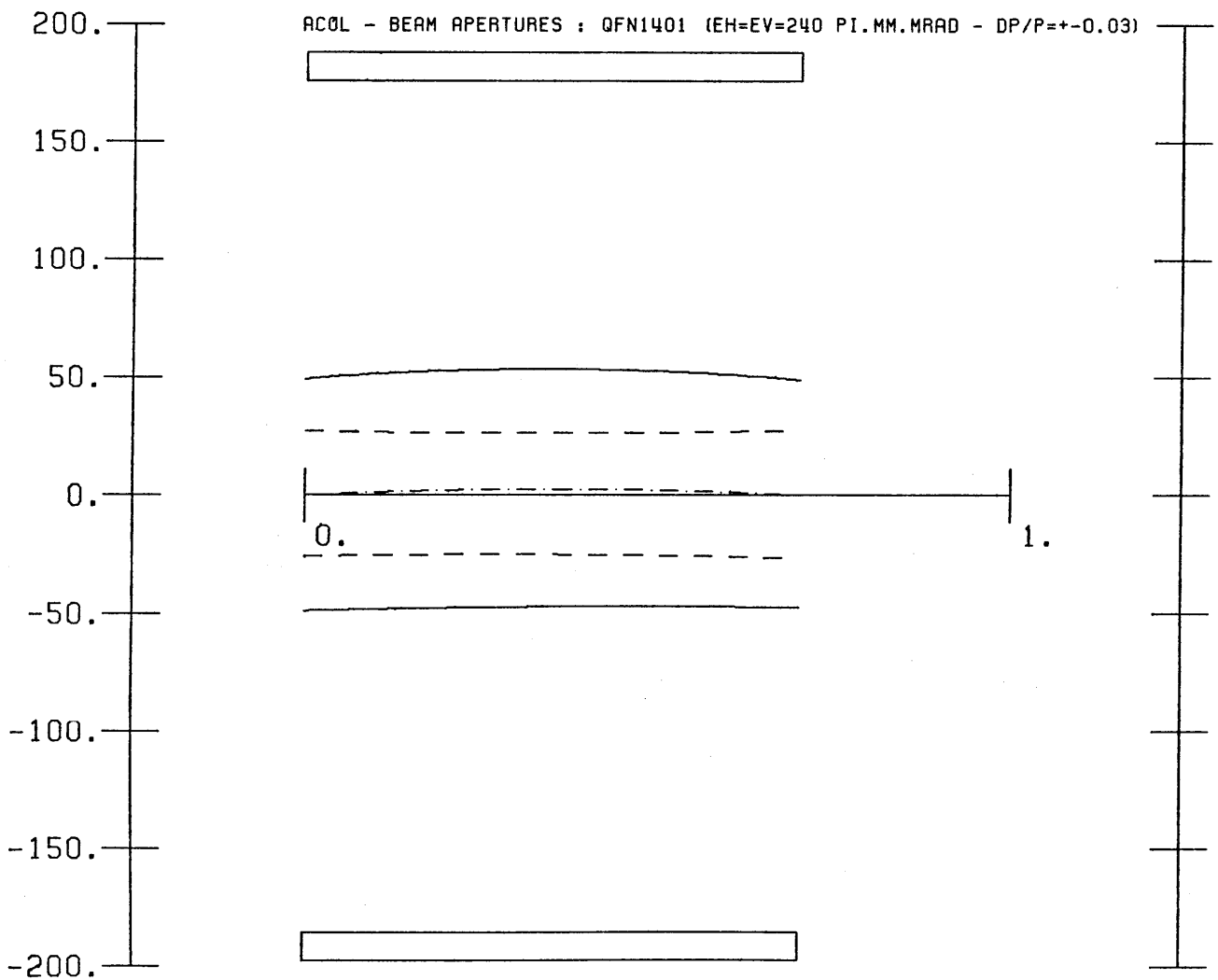
ACOL - BEAM APERTURES : QFN1401 (EH=EV=240 PI.MM.MRAD - DP/P=+-0.03)
200.
150.
100.
50.
0.
-50.
-100.
-150.
-200.
0.
1.

Fig. 28

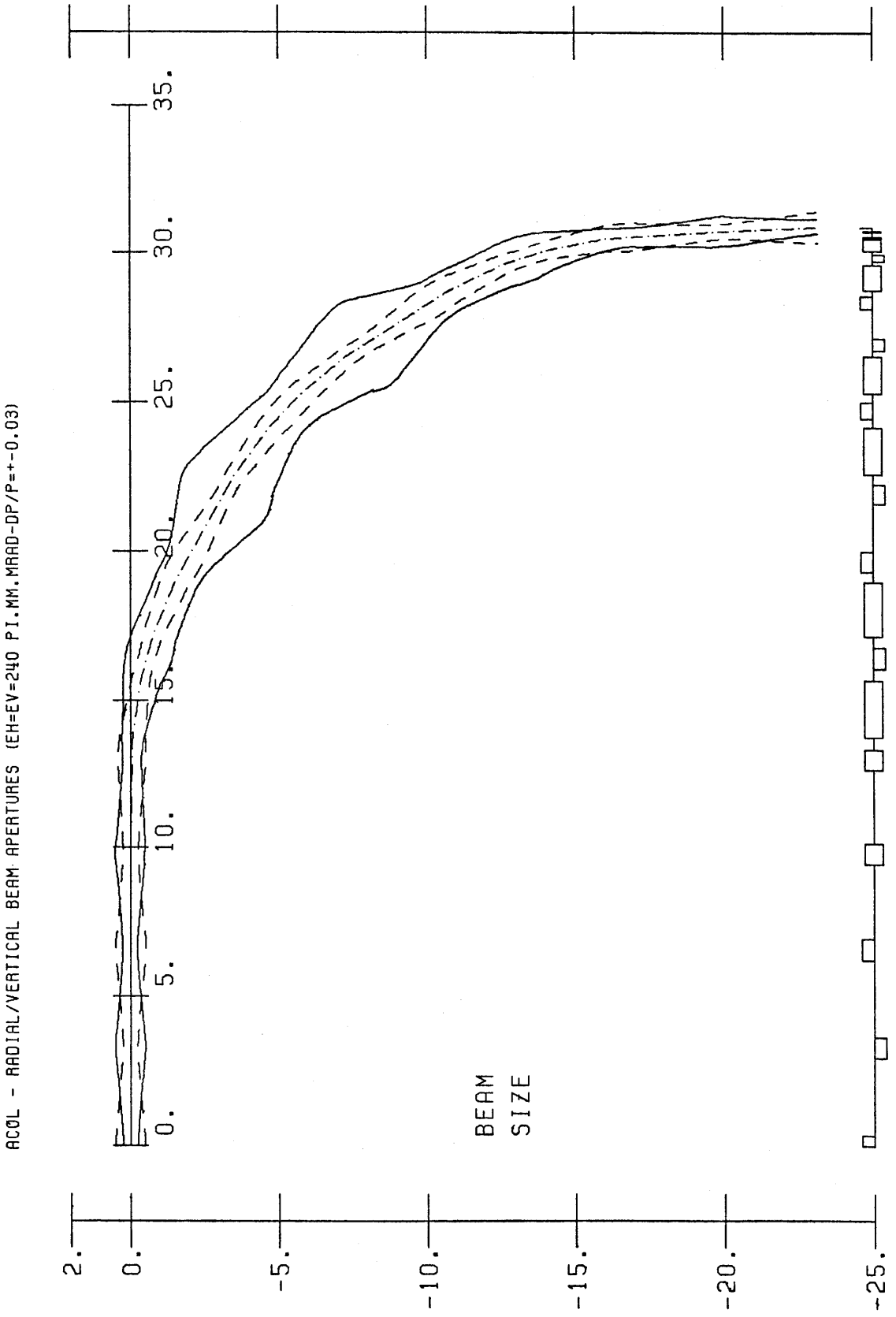

Fig. 29

Horizontal/vertical beam sizes around the ACOL ring and machine geometry.

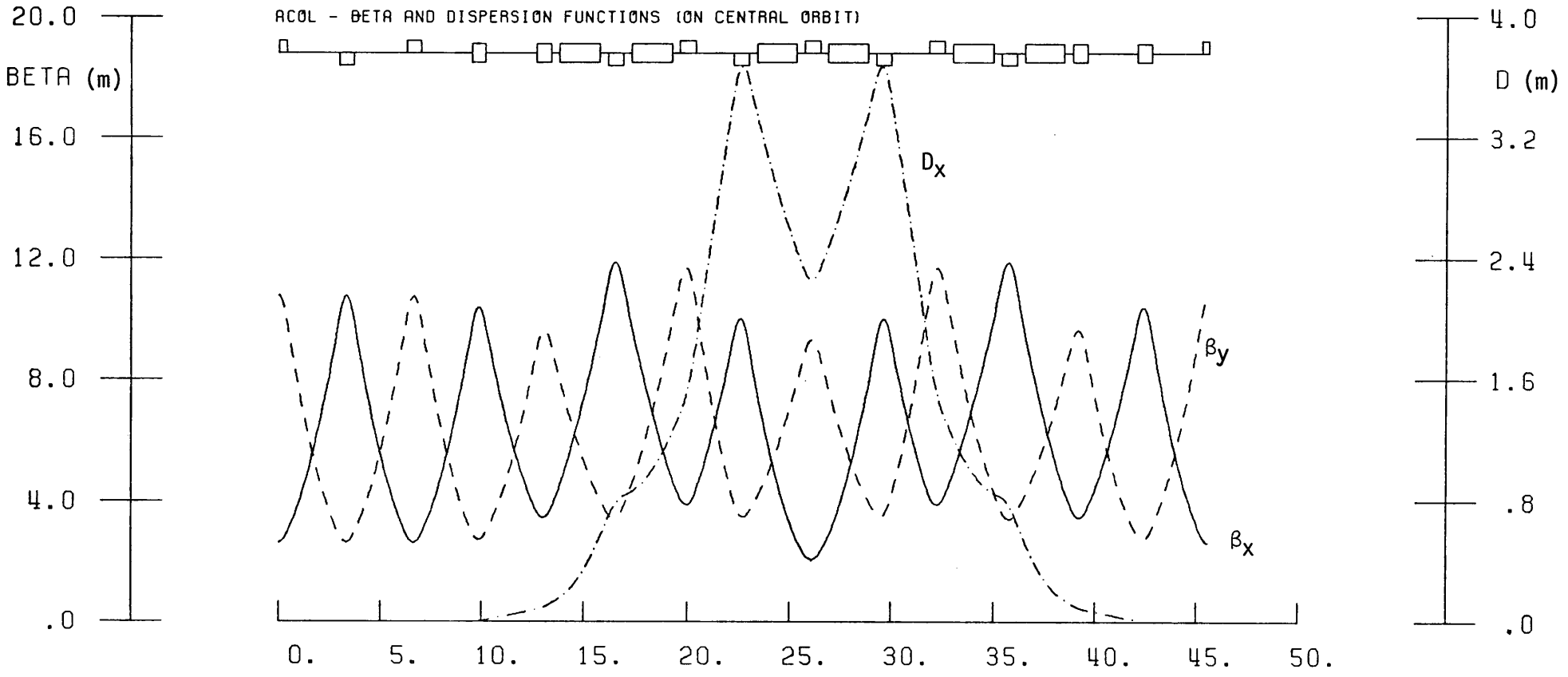

Fig. 30
ACOL characteristic functions